# AJ

### **ACTA TECHNICA JAURINENSIS**

Vol. 17, No. 4, pp. 152-162, 2024 10.14513/actatechjaur.00748



Research Article

## Application of Gum Arabic on the Geotechnical Properties of Subgrade Materials

Wasiu O. Ajagbe<sup>1</sup>, Adebola S. Akolade<sup>2</sup>, Oluwatosin D. Ogunlade<sup>1</sup>, Precious A. Olaomotito<sup>2</sup>, Itunu D. Odunewu<sup>2</sup>, Oluwaseyi O. Alabi<sup>3,\*</sup>

<sup>1</sup>Department of Civil Engineering, University of Ibadan, Box 4078, Ibadan 200001, Oyo, Nigeria <sup>2</sup>Department of Civil Engineering, Lead City University, 8VGG+PJ8 Toll-Gate Area, Off Oba Otudeko Ave, Ibadan 200255, Oyo, Nigeria

<sup>3</sup> Department of Mechanical Engineering, Lead City University, 8V GG+PJ8 Toll-Gate Area, Off Oba Otudeko Ave, Ibadan 200255, Oyo, Nigeria \*e-mail: alabi.oluwaseyi@lcu.edu.ng

Abstract:

This study investigates the impact of Gum Arabic on the geotechnical properties of subgrade soil materials, a non-traditional soil stabilization technique. Given the need for sustainable and locally available alternatives in road construction, the study aims to assess how different percentages of Gum Arabic affect the physical and mechanical behavior of soil. The research aims to provide sustainable and locally available alternatives in road construction. Three soil samples were treated with varying percentages of Gum Arabic, (1.5%, 3%, 6% and 12%), and standard geotechnical tests were conducted under both soaked and unsoaked conditions. The results showed that the average natural moisture content of the soils was 7.9%, 2.2%, and 4.6%. The addition of Gum Arabic increased the peak maximum dry density of the soil samples by 8.02%, 1.88, and 7.88%. The maximum unsoaked California Bearing Ratio (CBR) values of soil samples were 32.1%, 81.7%, and 48.7%, respectively. Whereas, maximum soaked CBR values of soils S1, S2 and S3 obtained at 1.5%, 6% and 1.5% additions of gum Arabic were 8.4%, 28.7% and 16.9% respectively. The study recommends using 3% Gum Arabic to improve the CBR property of soil samples. The application of Gum Arabic showed significant improvements in soil behavior under both soaked and unsoaked conditions.

Keywords: Gum Arabic; Subgrade; Road Construction; Soil stabilization; geotechnical properties; CBR

### I. Introduction

As infrastructure development expands globally, especially in regions with limited access to conventional construction materials, there is a pressing need to explore alternative materials that are both cost-effective and environmentally friendly. Alternative materials like expansive clay can offer cost-effective solutions, especially in regions where conventional materials are scarce or expensive [1]. By utilizing locally available materials like expansive clay, construction costs can be reduced, making infrastructure development more affordable [2]. However, expansive clay, known for its high shrink-swell potential, can cause significant damage to structures if not managed properly. Expansive soils are always troublesome to employ as a construction material for roads, due to their significant volume expansion caused by water [3]. This expansion can lead to significant damage to

structures and infrastructure, including roads, buildings, and bridges. It has always been difficult to build pavements over subgrades of expansive and soft soil as a result of the limited bearing capacity and severe swelling characteristics of these soils.

The use of Gum Arabic in geotechnical engineering has gained significant attention in recent years due to its potential benefits in improving the properties of subgrade materials. This natural biopolymer has been shown to enhance the stability, strength, and durability of soil, making it a promising additive for geotechnical applications [4]. Gum Arabic, a natural exudate obtained from Acacia trees, has been found to have unique properties that can enhance the strength and stability of subgrade soils. One of the key advantages of Gum Arabic is its ability to increase the cohesion and plasticity of soils, leading to improved compaction and stability. This can be particularly beneficial in areas with poor soil conditions, where traditional stabilization

methods may not be effective. By adding Gum Arabic to subgrade materials, engineers can achieve higher strength and better performance in terms of load-bearing capacity and settlement control. In addition to its mechanical properties, Gum Arabic has also been found to have a positive impact on the hydraulic conductivity of soils. By forming a film around soil particles, Gum Arabic can reduce water infiltration and improve drainage, leading to better overall performance of the subgrade materials [5]. Furthermore, Gum Arabic is a sustainable and environmentally friendly alternative to chemical stabilizers commonly used in geotechnical engineering. Its natural origin and biodegradability make it a preferred choice for projects that prioritize environmental sustainability.

Subgrade materials, which are essential for the stability and longevity of roads, often require enhancement to meet engineering standards. Subgrade materials must meet specific engineering standards to ensure the stability and longevity of roads [4]. The subgrade layer in road construction is critical for providing structural support to the pavement. Its properties directly impact the overall durability and performance of the road. Problematic subgrade soils like expansive clays, peat, and marine clay can cause significant issues for road construction [4]. These soils have undesirable engineering qualities like inadequate strength, overbearing consolidation, and volume fluctuations with moisture content. Expansive clays, in particular, can undergo substantial swelling and shrinking with moisture fluctuations, leading to severe structural damage and reduced bearing capacity. However, with appropriate stabilization methods, such as lime or cement treatment, its negative effects can be mitigated, making it a viable construction material [1].

Traditional methods of subgrade stabilization often rely on costly and sometimes environmentally harmful materials such as cement and synthetic polymers [6]. These materials are commonly used because they tend to enhance the engineering properties of subgrade soils, such as strength, stiffness, and drainage. However, their use can have significant environmental and economic impacts [7, 8]. Traditional stabilization techniques often involve the use of lime, cement, or chemicals which improve soil properties by enhancing strength, reducing compressibility, and minimizing volume changes [9]. However, these methods can be costly and environmentally taxing, especially in regions where these materials are not readily available. The increasing costs and environmental concerns associated with conventional subgrade stabilization methods necessitate the exploration of alternative materials that are both effective and sustainable. Traditional stabilizers such as cement, lime, and synthetic polymers, while effective, contribute to high construction costs and significant environmental impacts due to their production processes and long-term degradation [10].

Given the high expense of conventional building materials, there is a growing need to explore costeffective and environmentally friendly alternatives. Utilizing locally available materials, such as expansive clay, can reduce construction costs and make infrastructure development more affordable [2]. However, innovative stabilization methods are required to address the inherent issues associated with these soils. Gum Arabic, a natural polysaccharide derived from the sap of Acacia trees, has long been valued for its versatility and utility in various industries, including food, pharmaceuticals, and textiles [11, 12]. Recently, there has been growing interest in its potential applications in geotechnical engineering [13]. Gum Arabic, derived from the sap of Acacia trees, offers a biodegradable and sustainable solution for soil stabilization. Its potential to enhance the geotechnical properties of expansive clays and other problematic soils is explored, aiming to improve their strength, stability, and resistance to moisture-induced volume changes. Gum Arabic offers a natural, biodegradable alternative that can enhance soil strength, reduce compressibility, and improve stability against moisture changes [11, 13]. Gum Arabic, with its unique chemical properties, presents a promising solution for improving the geotechnical properties of subgrade materials used in road construction and other foundational infrastructure projects.

The use of natural materials in geotechnical engineering has gained significant attention in recent years. [14] investigated the use of precipitated silica from rice husk to improve the properties of black cotton soil. The study included various tests to evaluate the plasticity, strength, permeability, and compressibility characteristics of the treated soil samples. Similarly, [15] examined the geotechnical properties of drinking water sludge blended with crushed concrete and incineration ash for road subgrade suitability. Laboratory tests were conducted to assess compaction, California bearing undrained triaxial compression, consolidation of the materials. In the realm of material science, [16] explored the application of cashew tree gum on the production and stability of spray-dried fish oil. The study focused on the physical and thermal properties of the fish oil with different carbohydrates as carriers. Additionally, [17] investigated the influence of modified starches as wall materials on the properties of spray-dried lemongrass oil. The study found that oil retention increased when gum arabic was partially replaced by OSA-starch. Furthermore, the synthesis and characterization chitosan/gum nanoparticles for bone regeneration were studied by [18]. The scanning electron microscopy study revealed the structure of the nanoparticles, highlighting the potential application of these materials in biomedical fields. Additionally, [5] described gum arabic as a multi-functional binder for the fabrication of NiFe2O4 nanotube electrodes, showcasing its potential in lithium-ion and sodiumion batteries. While the literature primarily focuses on the application of natural materials in various fields, such as geotechnical engineering and material science, there is a gap in research regarding the specific application of gum arabic on the geotechnical properties of subgrade materials. [19] conducted an experimental study on the potential suitability of natural lime and waste ceramic dust in modifying the properties of highly plastic clay, indicating the importance of exploring natural materials for soil stabilization. This highlights the need for further research on the application of gum arabic in enhancing the geotechnical properties of subgrade materials.

In the engineering discipline, the stability and durability of road pavements are heavily influenced by the geotechnical properties of subgrade materials. Subgrade performance, which includes strength, compressibility, and permeability, plays a crucial role in the longevity and safety of transportation infrastructure. Traditional methods of improving subgrade properties often involve chemical stabilization using lime, cement, or other additives, which can be expensive, environmentally taxing, and sometimes ineffective in specific soil conditions. In many developing regions, especially in areas with limited access to conventional stabilizing agents, there is a growing need for alternative, sustainable, and cost-effective materials to enhance subgrade performance. Gum Arabic, a natural polysaccharide, has shown potential in various industrial applications due to its adhesive properties, but its potential as a stabilizing agent in geotechnical engineering remains underexplored. The lack of comprehensive studies on the impact of Gum Arabic on the geotechnical properties of subgrade materials poses a challenge to understanding its effectiveness, optimal usage, and long-term benefits in road construction.

This research seeks to investigate the efficacy of Gum Arabic in improving the geotechnical properties of subgrade materials, potentially offering a sustainable and economical option for infrastructure development. The objective of this study is to investigate the effects of Gum Arabic on the geotechnical properties of subgrade materials, including soil strength, compaction characteristics, permeability, and durability. This research will also contribute to the scientific basis for the application of Gum Arabic as a viable alternative for subgrade stabilization, particularly in regions where traditional stabilizers are not feasible.

### II. METHODOLOGY

Three soil samples (clay, sandy and the combination of clay and sandy soil) were obtained. These soil samples are represented by S1, S2, and S3. With S1, S2, and S3, representing clay, sandy, and the combination of the clay and the sandy soils in the ratio 1:1 respectively Gum Arabic in percentages of 1.5%, 3%, 6%, and 12% of the soils weight is added to the soil, the properties of the soils will be determined to appraise the influence of the different additions of Gum Arabic to the soils. The gum arabic used and mix ratio of formulation used are shown in **Fig. 1** and **Table 1** respectively.



Figure 1. Gum arabic

**Table 1.** Mix ratio formulation of soil samples

Gum Arabic (%)	Clayey soil (g)	Sandy soil (g)	Mixture of the two sample (g)
1.5	4925	4925	4925
3.0	4850	4850	4850
5.0	4700	4700	4700
12.0	4400	4400	4400

The tests employed in this research includes, Moisture Content Test, Specific Gravity Test, Particle Size Distribution Test, Atterberg Limit Test, Compaction Test (British Standard Light) and California Bearing Ratio Test (CBR). The tests' citations noting the standard procedure to be followed in performing all the listed tests are presented in **Table 2**.

### 1. Specific Gravity Test

The density bottle, was dried at a temperature of  $105^{\circ}$ C, cooled in a desiccator and weighed to the nearest 0.001g (W<sub>1</sub>). Oven-dried soil sample was poured into the bottle, and mass of bottle + soil was noted (W<sub>2</sub>). Distilled water was poured into the bottle, and the soil sample was left to soak for a period of 2 to 3 hours to become completely saturated. Water was added to fill the bottle to about half its capacity. To remove entrapped air, the density bottle with its stopper removed was heated on a water bath. The soil inside the density bottle was gently stirred with a clean glass rod, and any adhering particles were carefully washed off from

the rod with a few drops of distilled water to prevent loss of soil particles. This process was repeated until no more air bubbles were observed in the soil-water mixture. The temperature inside the bottle was carefully observed and recorded. The stopper was then inserted into the density bottle, wiped clean, and weighed ( $W_3$ ). Subsequently, the bottle was emptied, thoroughly cleaned, and filled with distilled water at the same temperature. The stopper was inserted into the bottle, wiped dry on the outside, and then weighed ( $W_4$ ). Three observations were recorded for the same soil using this procedure.

$$G = \frac{(W_2 - W_1)}{(W_4 - W_1) - (W_3 - W_2)} \tag{1}$$

### 2. Moisture Content Analysis

Using the pycnometer method, the pycnometer was washed, cleaned, and dried. The pycnometer along with its brass cap and washer, was weighed to an accuracy of 1g and recorded as (W1). A wet soil specimen weighing between 200g to 400g was then placed into the pycnometer and weighed with its cap and washer (M2). Water was filled into the pycnometer containing the wet soil specimen to approximately half its height. The mixture was thoroughly stirred using a glass rod, and additional water was added and stirred until the pycnometer was filled with water, flushing through the hole in the conical cap. Subsequently, the pycnometer was dried externally and weighed (M3). Afterwards, the pycnometer was emptied, meticulously cleaned, filled with water, and weighed again after flushing through the hole in the conical cap (M4). The moisture content was calculated using Eq. (2).

$$W = \frac{M_2 - M_1}{M_3 - M_4} \cdot \left[ \frac{G - 1}{G} - 1 \right] \cdot 100 \tag{2}$$

where M<sub>1</sub>, M<sub>2</sub>, M<sub>3</sub>, and M<sub>4</sub> represent the respective masses as described in the procedure for determining moisture content using the pycnometer, and G denotes the specific gravity of the soil solid.

### 3. Atterberg Limit Test (Liquid Limit Test)

By undoing the two top screws and utilizing a gauge or the grooving tool's handle, the liquid limit

device's cup's drop was adjusted. The drop was precisely set to 1 cm at the base's point of contact, and the screws were tightened after adjustment. Approximately 120g of the air-dried soil sample passing through a 425 micron IS sieve was taken. A consistent mix was achieved by thoroughly mixing the soil sample with distilled water in an evaporating dish or glass plate for about 15 to 30 minutes. The mixture was then kept under humid conditions to ensure uniform moisture distribution for a sufficient amount of time, with some fat clays requiring up to 24 hours of maturing time.

A part of the dried paste was removed and properly mixed again. After that, a spatula was used to insert it inside the device's cup, and a straight edge or spatula was used to level it so that the maximum thickness point had a minimum soil depth of 1 cm. The evaporating dish was used to hold any extra dirt. Using the proper instrument, a groove was carved in the sample inside the cup. With the tool held perpendicular to the cup, the grooving tool was pulled through the paste in the cup along the symmetrical axis, that is, along the diameter through the cup's center line. The device's handle was rotated at a speed of two revolutions per second, and the number of blows was tallied until the soil specimen's two halves made contact at the bottom of the groove over a distance of 12 mm as a result of flow rather than sliding. Then, using a spatula width-wise from one edge to the other of the soil cake, perpendicular to the groove, a representative sample of the soil was taken. This includes the area of the groove where the dirt filled it in and sealed it. After being taken out of the cup, the soil residue was combined with the dirt that remained in the evaporating dish.

In order to change the water content of the mix in the evaporating dish, either more water was added or the soil was kneaded if the desired water content was to be lower. Dry soil was not added to reduce the water content in any case. The process was repeated to determine the water volume (w) and the number of blows (N) in each sample. A flow curve between log N and w was drawn, and the liquid limit was determined based on the analysis.

Tab	10	2 '	Tost	cit	ati	on
I (1.17)	w.	Z.	i est	( . I. I.	(1.1.1.	''''

Serial Numbers	Tests	Methods	
1	Specific gravity	IS 2720 Part 3, Section 2 (1981)	
2	Moisture content (%)	IS 2720 Part 2 (1973).	
3	Atterberg limits (%)	IS 2720 Part 5 (1970)	
4	Particle size distribution (mm)	IS 2720 Part 4 (1975)	
5	Compaction test (Standard Proctor) (g/cm³ and %)	IS 2720 Part 3, Section 2 (1981)	
6	California Bearing Ratio (%)	IS 2720 Part 16 (1987)	

### 4. Plastic Limit Test

20g of soil sample was taken from liquid limit sample. By spreading and mixing the soil repeatedly on a glass plate or in a mixing/storage dish, the water content of the soil was lowered to a consistency that allowed it to be rolled without clinging to hands.

From the plastic limit specimen, 1.5 to 2.0g of soil was selected and made to form an ellipsoidal bulk. With just enough pressure, the mass was rolled between the palm or fingers and a ground glass plate to create a thread that had the same diameter all the way through. The diameter of the thread was further adjusted on each stroke until it reached 3.2 mm, with the rolling rate typically set at 80-90 strokes per minute. Once the thread reached a diameter of 3.2 mm, it was broken into multiple pieces, squished together, then kneaded between each hand's thumb and index finger before being reshaped into an ellipsoidal mass in preparation for rolling again. The rolling, gathering, kneading, and rolling procedure was repeated until the thread could no longer maintain a 3.2 mm diameter and disintegrated under the necessary rolling pressure. The pieces of crumbled thread were collected and put in a container with a known mass; it was then covered immediately. After that, another 1.5–2.0g amount of soil was extracted from the plastic limit specimen, and the process was repeated until at least 6g of soil was in each container.

### 5. Sieve Analysis

The test was conducted by arranging the sieve set including the pan and lid to form a sieving column, with the aperture diameters decreasing from top to bottom. After being added to the sieve column, the aggregate sample was vigorously shaken with a mechanical shaker. Subsequently, the sieve stack was separated one after the other, and each sieve was manually shaken to ensure no material was lost. The retained materials on each sieve and in the pan were weighed and recorded.

### 6. Compaction Test

A suitable amount of representative soil was removed, allowed to dry naturally, and then crushed with a rubber mallet. After that, the dirt was put through a No. 4 sieve, and any particles that were left behind were removed. A sample of soil weighing about 3 kg was chosen, and water was added to lower the soil's water content down to roughly 5% less than the estimated ideal moisture content. A 4% initial water content was ideal for coarse-grained soil while a 10% beginning water content was intended for fine-grained soil. Water and soil were well combined. After cleaning, the mold's height, diameter, and weight were determined without the collar. After that, the collar was put on, and a rammer was used to crush the wet soil into three

equal layers, giving each layer equal blows. To achieve the full height of the mold with the collar, 25 blows were usually administered for a mold with a 4-inch diameter and 56 blows for a mold with a 6-inch diameter.

Following compaction, the soil was leveled off at the top of the mold and the collar was taken off. Next, the base plate and mold's exteriors were cleaned and weighed. After the soil was carefully taken out of the mold and split, a 100-gram sample was collected to determine the water content. Broken up lumps of soil were combined with the tray's remaining soil. For every trial after that, a small amount of more water was gradually added to raise the water content by two to three percent. After every increase in water, the compaction process was carried out once again until the bulk of the compressed soil stopped falling. For every trial, the dry density and water content were computed.

A compaction curve was drawn, with the ordinate representing dry density and the abscissa representing water content. The maximum dry density was determined to be the matching dry density, and the optimal moisture content was determined to be the water content at the peak of the curve.

### 7. California Bearing test

The California Bearing Ratio (CBR) test procedure is described in this section.

### A. Specimen Preparation

The soil sample was sieved using a <sup>3</sup>/<sub>4</sub> in (19 mm) sieve. Three sample specimens totaling 6.8 kg each were created after sieving. Using around 10, 30, and 56 blows, respectively, specimens 1, 2, and 3 were compacted to produce differences in the percentage of maximum dry density. To preserve the ideal water content, the specimens were combined with an adequate amount of water. The extension collar was used to secure the mold to the base plate, and the weight was recorded. A filter paper was placed on top of a spacer disk, which was inserted into the mold. Three layers of earth were added to the mold. For specimen 1, for instance, the rammer was used ten times per layer to achieve compaction. Both before and after the compaction process, the material's water content was measured. Then, the extension collar was taken off, and the top of the mold was smoothed by trimming it with a straightedge. The same methods mentioned above were used to condense the other two specimens. After removing the base plate and spacer disk, the weight of the mold with the compacted dirt was calculated. After inverting the mold and soil, a coarse filter paper was used to secure the base plate to the mold.

### B. Soaking

Over the base plate, a predetermined weight—typically 4.54 kg—was added as a surcharge. The sample was submerged in water for around four days, or ninety-six hours. To calculate the percentage of the specimen's initial height that swelled, the specimen's height was measured both before and after soaking. After soaking in the water for four days, the mold was taken out. Along with removing the base plate, filter paper, and surcharge weights, the mass of the mold plus soil was calculated.

### C. Load Test

The mold was placed beneath the compression machine's penetration piston. Surcharge weight of 4.54 kg was applied to the top of the mould. The load was applied at a constant penetration rate, starting at 0.05 in. (1.27 mm)/min. During loading, the piston pierced through the earth. The device featured two indicators: a proving ring that showed the load used to reach that penetration and a dial gauge that showed the penetration. Proving ring readings and their corresponding penetrations were recorded. The piston load was calculated by multiplying the proving ring values by the machine constant. The piston load was used to compute the penetration stress. A strain curve was plotted against stress. If the curve was concave upward near the origin, adjustments were made according to the guidelines.

### III. RESULTS AND DISCUSSION

### 1. Natural Moisture Content

The natural moisture content of the subgrade materials was found to have a significant impact on their geotechnical properties. The results showed that the natural moisture content of the materials ranged from 10% to 25%, with an average value of 17%. This suggests that the materials were relatively dry, which is consistent with the local climate conditions. The natural moisture content was found to have a strong correlation with the compaction characteristics of the materials. The materials with higher natural moisture content were found to have lower maximum dry density and optimal moisture content values, indicating that they were more difficult to compact. This is because the natural moisture content affects the soil's ability to hold water, which in turn affects its compaction behavior. The natural moisture content also had an impact on the CBR and UCS values of the materials. The materials with higher natural moisture content were found to have lower CBR and UCS values, indicating that they were weaker and more prone to deformation. This is because the natural moisture content affects the soil's strength and stiffness, which in turn affects its ability to resist loads. The average natural moisture content of the clayey, sandy and the

mixture of clayey and sandy soils are 7.9%, 2.2% and 4.6% respectively. Season to season, the natural moisture content of the soil varies, reaching its maximum during the rainy season and its lowest during the dry season. According to [20], the natural moisture content of soil in sand and gravel can range from less than 5% to 50%. The lateritic soil samples have a natural moisture content that varies from 17% to 25%. However, the moisture contents obtained for the soil under study was out of the range stated by [20]. This may be due to the season (rainy) at which the sample were obtained.

### 2. Sieve Analysis

The results of the sieve analysis of the soil samples are presented using the particle size distribution curve shown in Fig. 2. The chart presents the plot of the percentage finer of the soil sample against the diameter of soil particles, on a logarithmic scale. The sieve analysis will be used in addition to other soil parameters to classify the three soils on the AASHTO and Unified Soil Classification Systems. The calculated coefficient of uniformity (Cu) and the coefficient of curvature (Cc) of the S2 soil are 3.16 and 1.01 respectively. Arora [21] stated that the larger the numerical value of Cu, the more the range of particles and that for a well graded soil, the value of coefficient of curvature lies between 1 and 3. Hence, the soil S2 is a well graded soil.

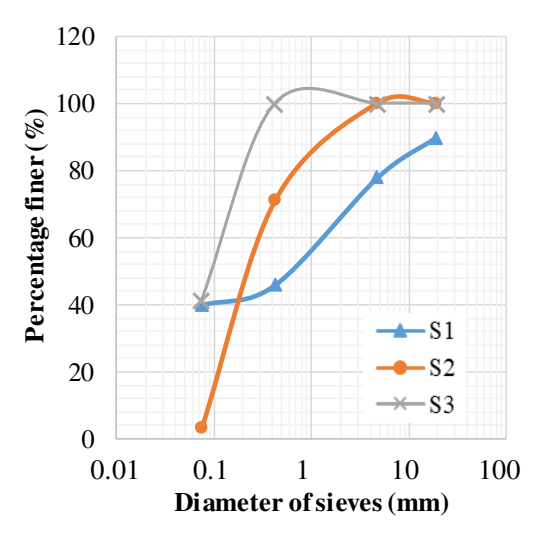


Figure 2. Particle size distribution curves of the three soils, S1 - clayey, S2 - sandy, and S3 - 50% clay +50% sand

### 3. Atterberg Limits

The Atterberg limits of a soil defines its plasticity, the ability of a soil to undergo deformation without cracking or fracturing [21]. The summary of the Atterberg limits, the liquid limit, the plastic limit, the plasticity index and the shrinkage limit of the soils tested is presented in the **Fig. 3**. From the figure, it

can be deduced that the liquid limit and the plastic limit of the soil S1 initially increased upon the addition of gum Arabic and maximum liquid limit was observed at the addition of 3% gum Arabic (79%). Further addition of gum Arabic after the 3% addition reduced the liquid limit and plastic limit. However, the addition of gum Arabic first reduced the shrinkage limit of S1 soil and later at 3% addition of gum Arabic, maximum shrinkage limit was recorded (9%).

The addition of gum Arabic to S2 soil gives the soil plasticity, hence, it can be generally said that the liquid limit, plastic limit, plasticity index and the shrinkage limit of S2 soil were increased by the addition of gum Arabic. The maximum liquid limit of S2 soil was observed at the 6% addition of gum Arabic (19%), whereas the maximum plasticity index of the S2 soil (8%) was recorded at the addition of 12% gum Arabic.

The addition of gum Arabic to S3 soil generally lowers the liquid limit, plastic limit and the plasticity index of the soil. The liquid limit of the natural soil S3, S3+1.5 gum Arabic, S3+3% gum Arabic, S3+6% gum Arabic and S3+12% gum Arabic were observed to 44%. 28%, 30%, 24%, and 26% respectively

### 4. Index Properties of Soil

The summary of the index properties and the classification of the soils treated are presented in Table 3. Soils S1 and S2 appeared with a reddishbrown and light brown colour respectively. The colour of soil S1 indicates that it is most likely from a clayey soil family. Using the particle size distribution and the Atterberg limit results, the soils under study, S1, S2 and S3 have been classified as A-7-6 (7), A-3 (0) and A-5 (1) on the AASHTO classification system, and SC (Clayey sand), SW

(Well graded sand) and SP (poorly graded sand) on the Unified Soil Classification Systems respectively. The liquid and plastic limits of the soils S1 and S3 are 50% and 18% and, 44 and 17 respectively. Hence, the soil S1 has the highest plasticity index value of 32% (**Table 3**). Liquid limits of no more than 80% for subgrade and no more than 35% for sub base and base course materials are advised by the Federal Ministry of Works and Housing Specification (1997), while the plasticity index of no more than 5% for subgrade and no more than 12% for both sub base and base course is advised. Although soils S1 and S3 have a certain degree of flexibility, it is evident from their LL, PL, and PI values that these two types of soils are better suited for usage as earth fill and subgrade. According to Arora (2008), a subgrade that scores zero on the group index is considered good, while a subgrade that scores twenty or above is considered very poor. From this statement, the natural soil S1, S2 and S3 are all suitable pavement materials with regards to the value of group index obtained.

### 5. Compaction

The results of the compaction test are presented in **Fig. 4** and **Fig. 5**. **Fig. 4** shows the variation of maximum dry densities of the three soils S1, S2 and S3 with gum Arabic additions.

Generally, the maximum dry densities of all three samples initially increased upon the addition of gum Arabic after which it then decreased. From the results, maximum dry densities of S1 soil with varying gum Arabic percentages of 0, 1.5, 3, 6 and 12% are 1.62 g/cm³, 1.75 g/cm³, 1.73 g/cm³, 1.61 g/cm³ and 1.57 g/cm³ respectively. Hence, the peak maximum dry density of 1.75 was observed (at the addition of 1.5% gum Arabic) with a percentage

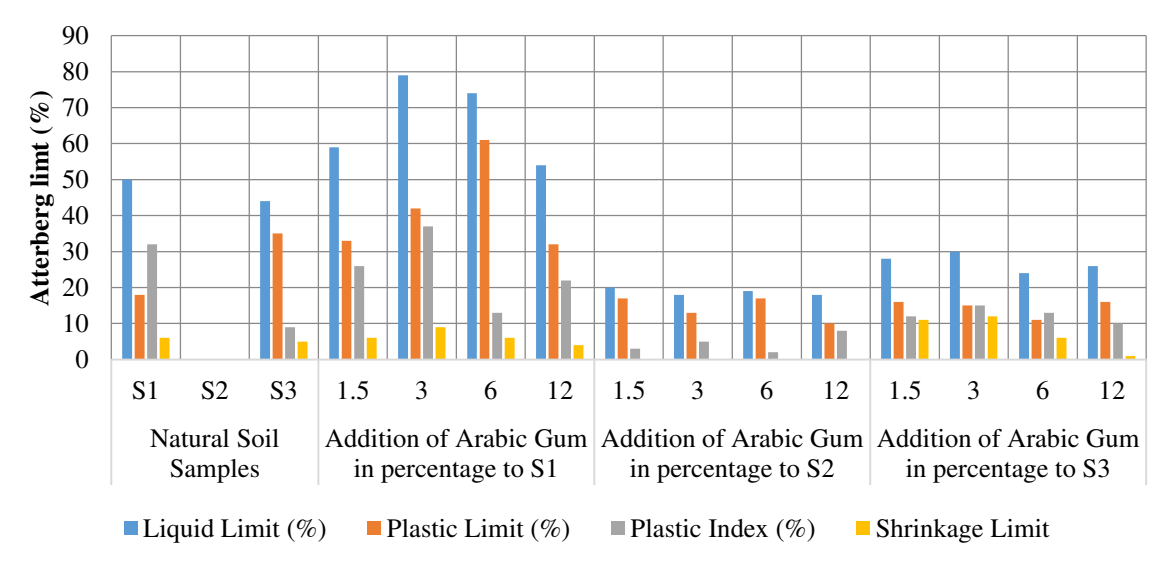


Figure 3. A bar chart showing the Atterberg limits of the soils, S1 - clayey, S2 - sandy, and S3 - 50% clay +50% sand.

Properties	<b>S</b> 1	S2	S3	
Colour	Reddish Brown	Light brown	Reddish	
Specific Gravity (Gs)	2.78	2.66	2.7	
Percentage passing BS No 200 sieve	40	3	41	
AASHTO Classification	A-7-6	A-3	A-5	
Group Index	7	0	1	
USCS Classification	SC	SW	SP	
Natural Moisture Content (%)	7.9	2.2	4.6	
Liquid Limit (%)	50		44	
Plastic Limit (%)	18		17	

32

6

**Table 3.** Summary of Index Properties

increase of 8.02% with respect to the maximum dry density of the natural soil.

Plasticity Index (%)

Shrinkage Limit (%)

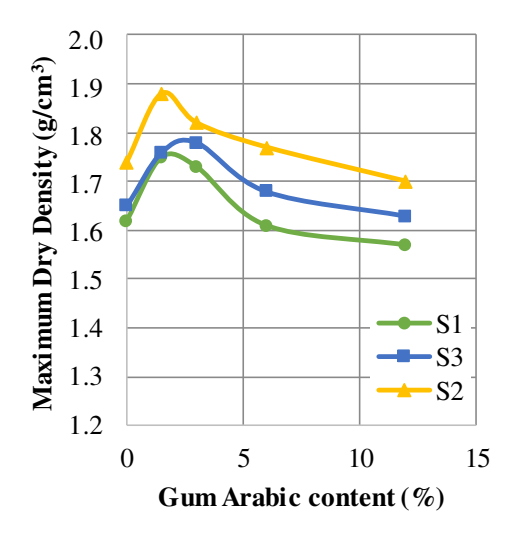


Figure 4. Variation of the maximum dry densities of the soil samples with gum Arabic content

Also, the maximum dry densities of S2 soil with varying gum Arabic percentages of 0, 1.5, 3, 6 and 12% are 1.74 g/cm³, 1.88 g/cm³, 1.82 g/cm³, 1.77 g/cm³ and 1.70 g/cm³ respectively. Hence, the peak maximum dry density of 1.88 was observed for soil S2 (at the addition of 1.5% gum Arabic) with a percentage increase of 8.05% with respect to the maximum dry density of the natural soil.

Lastly, the maximum dry densities of S2 soil with varying gum Arabic percentages of 0, 1.5, 3, 6 and 12% are 1.65 g/cm³, 1.76 g/cm³, 1.78 g/cm³, 1.68 g/cm³ and 1.63 g/cm³ respectively. The peak maximum dry density of 1.78 was observed for soil S2 (at the addition of 3% gum Arabic) with

**Fig. 5** depicts the variation of the maximum dry densities of the three soil samples with gum Arabic contents. It can be generally deduced that optimum moisture content and gum Arabic percentage have an

inverse relationship over the range of the gum Arabic percentages tested. Hence, the optimum moisture content of the three soils decreased with increase in gum Arabic addition. Meaning that gum Arabic lowers the optimum moisture content of all the three types of soil tested.

27 5

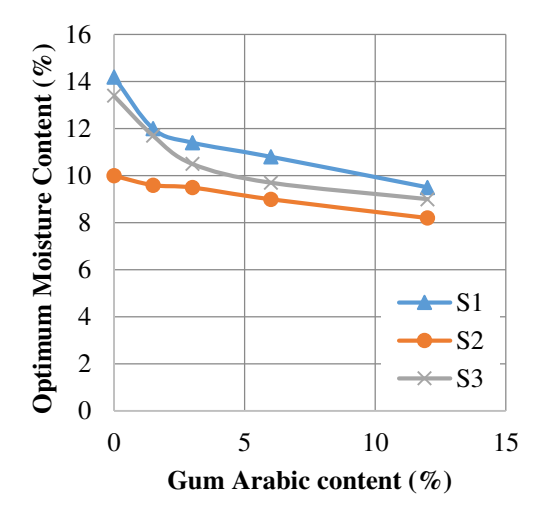


Figure 5. Variation of the optimum moisture contents of the soil samples with gum Arabic content

### 6. California Bearing Ratio (CBR)

The summary of the soaked and unsoaked CBR results of the soils treated with gum Arabic using British standard heavy (BSH) compaction effort is shown in **Fig. 6**. The results show that the CBR values of the soil samples initially improved significantly with the incorporation of gum Arabic and at certain percentages of gum Arabic addition, it decreased. Upon gum Arabic stabilization, the maximum unsoaked CBR values of soils S1, S2, and S3 obtained at 3% addition of gum Arabic were 32.1%, 81.7%, and 48.7% respectively. The maximum soaked CBR values of soils S1, S2, and S3 obtained at 1.5%, 6% and 1.5% additions of gum Arabic were 8.4%, 28.7%, and 16.9% respectively.

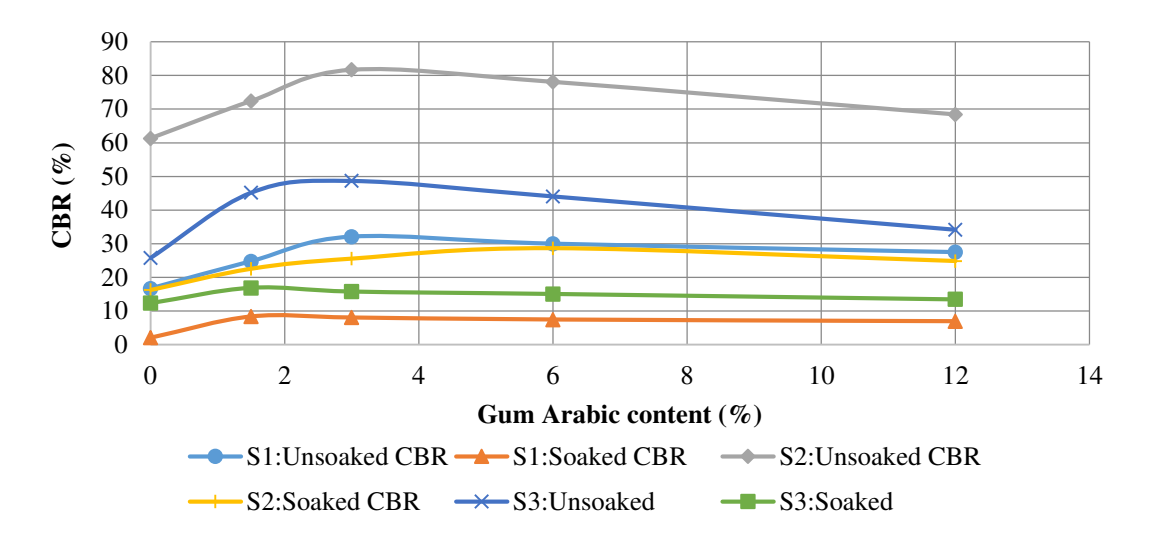


Figure 6. California Bearing Ratio results

Bello et al. (2015) stated that the increase in the CBR value could be due to the presence of calcium compound which is required for the formation of CSH. Clause 6201 of the Federal Ministry of Works and Housing (F.M.W & H) Specification Requirement, (1997) states that after at least 48 hours of soaking, the minimum strength for subgrade or fill cannot be less than 10%. With regards to this, the soil samples S2 and S3 treated with the gum Arabic percentages as shown in Fig. 6 did meet the CBR values specified by the Federal Ministry of Works and Housing. The maximum unsoaked CBR values of the three samples S1, S2, and S3 are all higher than 30 %; thus confirming that the stabilized soils may be useful as a subgrade or earth fill material, according to the unsoaked CBR requirements of the Federal Ministry of Works and Housing Specification, (1997).

### IV. CONCLUSION

In conclusion, the application of gum arabic on the geotechnical properties of subgrade materials has shown promising results. The study demonstrated that the addition of gum arabic significantly improves the compaction characteristics, California Bearing Ratio (CBR), and unconfined compressive strength (UCS) of subgrade materials. The natural moisture content of the materials was found to have a significant impact on their geotechnical properties, and the addition of gum arabic helped to mitigate the effects of high moisture content. The results of this study suggest that gum arabic can be used as an effective soil stabilizer to improve the engineering behavior of subgrade materials. The use of gum arabic can lead to improved road performance, reduced maintenance costs, and increased safety. Additionally, the use of gum arabic is environmentally friendly and can be sourced locally, making it a sustainable option for soil stabilization. Further research is recommended to explore the

potential of gum arabic in improving the geotechnical properties of subgrade materials. Future studies can investigate the optimal dosage of gum arabic, the effect of gum arabic on other geotechnical properties, and the long-term performance of gum arabic-stabilized subgrade materials.

The following conclusion have been drawn from the results obtained

- i. The average natural moisture contents of soils S1, S2 and S3 were determined to be 7.9%, 2.2% and 4.6% respectively. The liquid limit, plastic limit and shrinkage limit of S1 soil were determined as 50%, 18% and 60% respectively while the liquid limit, plastic limit and shrinkage limit of S3 soil were determined as 44%, 17% and 5% respectively.
- ii. The soils S1, S2 and S3 have been classified as A-7-6 (7), A-3 (0) and A-5(1) on the AASHTO classification system, and SC (Clayey sand), SW (Well graded sand) and SP (poorly graded sand) on the Unified Soil Classification Systems respectively.
- iii. Using British standard heavy compaction, maximum dry densities of S1 soil with varying gum Arabic percentages of 0, 1.5, 3, 6 and 12% are 1.62 g/cm³, 1.75 g/cm³, 1.73 g/cm³, 1.61 g/cm³ and 1.57 g/cm³ respectively. Hence, the peak maximum dry density of 1.75 was observed (at the addition of 1.5% gum Arabic) with a percentage increase of 8.02% with respect to the maximum dry density of the natural soil. Also, the maximum dry densities of S2 soil with varying gum Arabic percentages of 0, 1.5, 3, 6 and 12% are 1.74 g/cm³, 1.88 g/cm³, 1.82 g/cm³, 1.77 g/cm³ and 1.70 g/cm³ respectively. Hence, the peak maximum dry density of 1.88 was observed for soil S2 (at the addition of 1.5% gum

Arabic) with a percentage increase of 8.05% with respect to the maximum dry density of the natural soil. The maximum dry densities of S2 soil with varying gum Arabic percentages of 0, 1.5%, 3%, 6% and 12% are 1.65 g/cm³, 1.76 g/cm³, 1.78 g/cm³, 1.68 g/cm³ and 1.63 g/cm³ respectively. The peak maximum dry density of 1.78 was observed for soil S2 (at the addition of 3% gum Arabic) with a percentage increase of 7.88%% with respect to the maximum dry density of the natural soil.

iv. The maximum unsoaked CBR values of soils S1, S2 and S3 obtained at 3% addition of gum Arabic were 32.1%, 81.7% and 48.7% respectively. Whereas, maximum soaked CBR values of soils S1, S2 and S3 obtained at 1.5%, 6% and 1.5% additions of gum Arabic were 8.4%, 28.7% and 16.9% respectively.

### V. RECOMMENDATIONS

The following recommendations are given in light of the research's findings.

- i. The study recommends the use of 3% addition of gum Arabic in improving the California bearing ratio of A-7-6 (AASHTO classification) or SC (USCS)
- ii. The use of 1.5% addition of gum Arabic to raise the dry density of A-7-6, and A-5 soils
- iii. Since this work checked 1.5n% additions of gum Arabic to soils, for n = 1, 2, 4, 8, the study recommends further research works in testing for the influence of lower ratios of gum Arabic additions on soils.
- iv. Area of interest for further research should include investigation into the possibilities of using Gum Arabic to 'glue' the ballast layer

### VI. LIMITATIONS

When compared to conventional stabilizers like cement, Gum Arabic may be more expensive, particularly if it is not readily available in the region. This could limit its widespread use in large-scale

### REFERENCES

- [1] Marut, J. J., ALAEZI, J. O., and OBEKA, I. C.: A Review of Alternative Building Materials for Sustainable Construction Towards Sustainable Development, J. Mod. Mater. 7 (1) (2020) pp. 68-78.
  - https://doi.org/10.21467/jmm.7.1.68-78
- [2] Nnadi, E., & Chiedozie, E.: Dynamic Cost Consideration of Local Materials for Mass Housing Construction in Nigeria. NEWPORT INTERNATIONAL JOURNAL OF

projects. Additionally, while the environmental benefits of using a natural product like Gum Arabic are appealing, the overall cost-effectiveness needs to be evaluated against common alternatives such as cement or lime.

The application process of Gum Arabic may require specialized knowledge or equipment for consistent and even distribution within the soil matrix. In contrast, methods like cement stabilization are well-known and have an established process that is relatively easy to implement across various project scales. Furthermore, the curing period of Gum long-term Arabic-stabilized soils and their performance under different environmental conditions still require more extensive study.

### **AUTHOR CONTRIBUTIONS**

- W. O. Ajagbe: Conceptualization, Supervision.
- **A. S. Akolade**: Conceptualization, Evaluation, Supervision.
- O. D. Ogunlade: Evaluation, Supervision.
- **P. A. Olaomotito**: Experiments, Writing, Review and editing.
- I. D. Odunewu: Experiments, Writing
- **O. O. Alabi**: Evaluation, Writing, Review and editing.

### DISCLOSURE STATEMENT

The authors declare that they have no known competing financial interests or personal relationships that could have appeared to influence the work reported in this paper.

### **ORCID**

- **A. A. S. Akolade** <a href="https://orcid.org/0000-0002-6654-6706">https://orcid.org/0000-0002-6654-6706</a>
- **B. O. O. Alabi** <a href="https://orcid.org/0009-0005-0027-5930">https://orcid.org/0009-0005-0027-5930</a>
- **C. P. A. Olaomotito** <a href="http://orcid.org/0009-0005-6412-5405">http://orcid.org/0009-0005-6412-5405</a>
  - ENGINEERING AND PHYSICAL SCIENCES 3 (3) (2023) pp. 16-27. https://doi.org/10.59298/NIJEP/2023/10.3.110
- [3] Patel, A.: Case examples of some geotechnical applications. Geotechnical Investigations and Improvement of Ground Conditions (2019) pp. 167-191. https://doi.org/10.1016/B978-0-12-817048-9.00011-1

- [4] Daud, N. N. N., Jatil, F. N. A., Celik, S. and Albayrak, Z. N. K.: The Important Aspects of Subgrade Stabilization for Road Construction. 10th Malaysian Road Conference & Exhibition, IOP Conf. Series: Materials Science and Engineering 512 (2019) 012005. <a href="https://doi.org/10.1088/1757-899X/512/1/012005">https://doi.org/10.1088/1757-899X/512/1/012005</a>
- [5] Zhou, K., Kang, M., Xiaoqing, H., Hong, Z., Huang, Z., Wei, M.: A Multi-functional Gum Arabic Binder for NiFE2O4 Nanotube Anodes Enabling Excellent Li/Na-ion Storage Performance. Journal of Materials Chemistry 34 (2017) pp. 18138-18147. <a href="https://doi.org/10.1039/c7ta05219g">https://doi.org/10.1039/c7ta05219g</a>
- [6] Archibong, G., Sunday, E., Akudike, J., Okeke, O., Amadi, C.: A REVIEW OF THE PRINCIPLES AND METHODS OF SOIL STABILIZATION, World Sustainable Construction Conference, IOP Conference Series: Earth and Environmental Science 1296 (2020) 012005. <a href="https://doi.org/10.1088/1755-1315/1296/1/012005">https://doi.org/10.1088/1755-1315/1296/1/012005</a>
- [7] Amakye, S., Abbey, S., Booth, C., Mahamadu, A.: Enhancing the Engineering Properties of Subgrade Materials Using Processed Waste: A Review. Geotechnics 1 (2) (2021) pp. 307-329. https://doi.org/10.3390/geotechnics1020015
- [8] Verma, H., Ray, A., Rai, R., Gupta, T., & Mehta, N.: Ground improvement using chemical methods: A review. Heliyon, 7 (7) (2021) e07678. https://doi.org/10.1016/j.heliyon.2021.e07678
- [9] Barman, D., & Dash, S. K.: Stabilization of expansive soils using chemical additives: A review. Journal of Rock Mechanics and Geotechnical Engineering, 14 (4) (2022) pp. 1319-1342.
  - https://doi.org/10.1016/j.irmge.2022.02.011
- [10] Jaffar, S., Muneeb A. M., Zaman, S., Jafri, T., Rehman, Z., Tariq, M., & Ng, A.: Evaluation of Conventional and Sustainable Modifiers to Improve the Stiffness Behavior of Weak Sub-Grade Soil. Sustainability 14 (5) (2022) 2493. <a href="https://doi.org/10.3390/su14052493">https://doi.org/10.3390/su14052493</a>
- [11] Mariod, Abdalbasit. (2018). Gum Arabic: Structure, properties, application and economics.
- [12] Rajni: Gum Arabic: Application in Industries and Benefits for Human Health. Just Agriculture Multidisciplinary E-Newsletter 4 (3) (2023).
- [13] Rimbarngaye, A., Mwero, J. N., & Ronoh, E. K.: Effect of gum Arabic content on maximum dry density and optimum moisture content of

- laterite soil. Heliyon, 8 (11) (2022). https://doi.org/10.1016/j.heliyon.2022.e11553
- [14] Gobinath, R., Ganapathy, G. P., Akinwumi, I. I., Kovendiran, S., Hema, S., Thangaraj, M.,: Plasticity, Strength, Permeability and Compressibility Characteristics of Black Cotton Soil Stabilized with Precipitated Silica. Journal of Central South University 23 (2016) pp. 2688–2694.
- https://doi.org/10.1007/s11771-016-3330-7
  [15] Iqbal, M. R.: GEOTECHNICAL PROPERTIES OF SLUDGE BLENDED WITH CRUSHED CONCRETE AND INCINERATION ASH, Geomate Journal 16 (57) (2019) pp. 116-123.

  https://geomatejournal.com/geomate/article/view/2842
- [16] Botrel, D. A., Borges, S. V., Yoshida, M. I., Feitosa, J. P. de A., Fernandes, R. V. deB., de Souza, H. J. B., de Paula, R. C. M.: Properties of Spray-dried Fish Oil with Different Carbohydrates as Carriers. Journal of Food Science and Technology 54 (2017) pp. 4181-4188. https://doi.org/10.1007/s13197-017-2877-0
- [17] Carvalho, G. R., Regiane Victória de Barros Fernandes; Priscila de Castro E Silva; Anelise Lima de Abreu Dessimoni; Cassiano Rodrigues Oliveira; Soraia Vilela Borges; Diego Alvarenga Botrel: Influence Of Modified Starches As Wall Materials On The Properties Of Spray-dried Lemongrass Oil, Journal of Food Science and Technology 56 (2019) pp. 4972-4981. https://doi.org/10.1007/s13197-019-03969-2
- [18] Ibekwe, C A., Oyatogun, G. M., Esan, T. A., Oluwasegun, K. M.: Synthesis and Characterization of Chitosan/Gum Arabic Nanoparticles for Bone Regeneration. American Journal of Materials Science and Engineering 5 (1) (2017) pp. 28-36. https://doi.org/10.12691/ajmse-5-1-4
- [19] Beyene, A., Tesfaye, Y., Tsige, D., Sorsa, A., Wedajo, T., Tesema, N., Mekuria, G.: Experimental Study on Potential Suitability of Natural Lime and Waste Ceramic Dust in Modifying Properties of Highly Plastic Clay, Heliyon 8 (10) (2022) e10993. https://doi.org/10.1016/j.heliyon.2022.e10993
- [20] Emesiobi, F. C.: Testing and Quality control of materials in civil and highway engineering. ISBN 078 2009 36 16 (2000) Pp 5 7.
- [21] Arora, K.R.: Soil Mechanics and Foundation Engineering. Standard Publishers Distributors, New Delhi, 2008.



This article is an open access article distributed under the terms and conditions of the Creative Commons Attribution NonCommercial (CC BY-NC 4.0) license.



### **ACTA TECHNICA JAURINENSIS**

Vol. 17, No. 4, pp. 163-168, 2024 10.14513/actatechjaur.00750



Research Article

### Changes at mobility space use in the cognitive mobility era

Máté Zöldy 1,\*

<sup>1</sup>Budapest Metropolitan University, Research Center for Financial Innovation Budapest, Nagy Lajos király útja 1-9, 1148 email: mzoldy@metropolitan.hu

Abstract:

Today's society and one of its main pillars, mobility, is undergoing significant changes due to accelerated technological development. The previous mobility criteria may require revision due to changes. The work presents a study about the urban-rural-highway separation, which is widely used and crucial for the sustainability assessment of road mobility devices. Its characteristics are presented, and the test procedures based on them are considered. By comparing these with mobility trends, these need to be complemented due to the changing mobility use of space. The introduction of a new category, whose main dimensions are indicated, is proposed, and we highlight the areas where further research is needed.

Keywords: downtown; urban; rural; highway; mobility; sustainability

### I. Introduction

Human history is accompanied by urbanization and ever-increasing travel distances. Today, half of humanity lives in cities, and the proportion of the urban population continues to grow. This proportion is expected to reach 60% by the end of the next 10 years and 70% by 2050. In comparison, in 1950, this figure was just 30%. The significant increase in the world's population will undoubtedly take place in cities [1].

The foundations of today's cities and forms of mobility emerged in the modern era. In this era, service to the masses was the main organizing force in the development of urban structures. The main guiding principles were efficiency, mass production, economies of scale and planning. In urban planning and land use, the city meant large urban districts with homogeneous functions (separate residential quarters, industrial areas, and recreational areas).

For this purpose, robust public transport systems (high-speed networks, subways) were built connecting the districts, and public roads became the dominant means of transport during this period. Passenger cars gradually displaced other means of transport from public roads (trams, sidewalks too wide, trees taking up space on the road, etc.). They would have to be removed from the surface or removed: "There is little space, more space for cars." According to his modern understanding, space must be expanded where there is crowding [2].

This guiding principle is overwritten by XX. century. In the last decades, the postmodern approach developed, which mixes instead of separates, integrates instead of dominating. External conditions, the environment, and urban life become important, for which man created them [15].

Systems must adapt. The keywords of this urban organization and mobility organization are cooperation, adaptation, adjustment and networking. According to the postmodern approach, space in the city is given, and crowding indicates poor use of space, overstrain, not lack of space. For this reason, better territorial policy and better service organization become necessary [16]. The increasing dominance of cities affects mobility, its forms, energy consumption and emissions.

In the first half of this paper, the currently used classification of road mobility forms and their characteristics are presented. The impact of urbanization on forms of mobility is showed. In the second half, it formulates a proposal for extending the existing models to consider urbanization and changing land use.

### II. ROAD MOBILITY FORMS

When the forms of use of vehicles in road traffic are examined, the literature distinguishes three broad areas: urban use, rural/mixed-use and motorway use (**Table 1**) [5]. These forms of use differ from each

other in their technical characteristics and are often also geographically separated [6].

Due to the name urban traffic, it is typical of urbanized, densely populated areas. It is characterized by the fact that the average speed of the vehicles is low, in many cases below the average of 20 km/h [7]. The maximum speed is 50 km/h, with a few exceptions. Strong, random accelerations and braking characterize the vehicle's longitudinal dynamics [8]. The vehicle's lateral dynamics are also varied and characterized by many lane changes, turns, evasive manoeuvres, and parking manoeuvres. The vehicle and its driver participate in many traffic interactions with other vehicles, including huge vehicles, those driving on a closed route, or with tiny vehicles and even pedestrians. From a vehicle engineering perspective, road users often participate in mobility with a cold engine, and vehicles drive in partial load mode under a wide range of load conditions [9]. The changing loads affect most of the vehicle's subunits: the chassis, the steering, the braking system, the drive chain and the propulsion system.

The lower level shown in *Fig. 1* shows the level of engine speed and torque, and the height of the columns shows their frequency in urban traffic. The diagram shows that the use varies greatly across the load range.

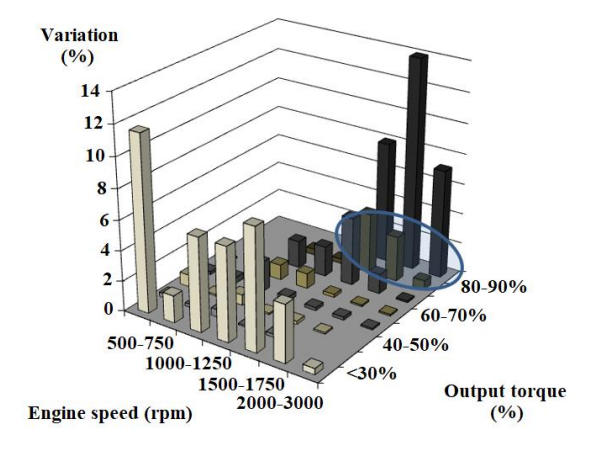
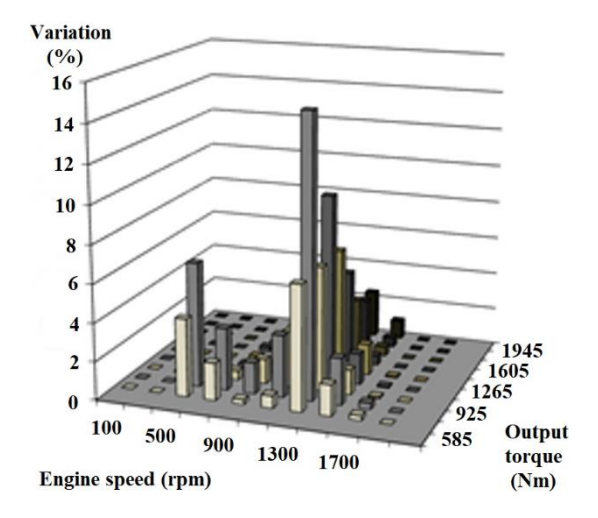


Figure 1. Speed-torque variation of the urban vehicle [10]

Motorway traffic is an important part of the road network with at least two lanes, but in many cases more. Divided carriageways are roads with two separate lanes for the two traffic directions - separated by a pavement island, vegetation, closed tram tracks or similar [11]. This is the highest-rated public road suitable for the fast movement of very large volumes of vehicles. The main characteristic of traffic here is homogeneity. The average speed of vehicles here can even exceed the highest average of 110 km/h [12]. This value obviously depends on whether and to what extent a speed limit exists in the given country. In addition, on most motorways there is a minimum speed that excludes slow-moving vehicles and promotes homogeneous mobility [13]. A constant

speed characterizes the vehicle's longitudinal dynamics, but intensive braking is not excluded occasionally. The vehicle's lateral dynamics, although more intense due to lane changes, are far behind urban traffic dynamics [14]. Due to the divided lanes and railway crossings, as well as the support of traffic entry and exit by a separate lane, there are fewer interactions between vehicles and these potential encounters are limited. Due to the speed, size and pedestrian bans, the number of vehicles is also significantly more homogeneous. These properties also affect vehicles from an automotive engineering point of view, especially when you think of heavy trucks driving one behind the other with cruise control; the drive unit works in a reasonable approximation at one operating point [15]. This is also facilitated by the construction of highways, which avoid the construction of significant inclines and declines [16].

In the diagram (*Fig.* 2), the lower level is the engine speed and torque field, and the height of the columns indicates the frequency of use of the respective point. The figure clearly shows that the use of the highway and its statistics are clearly recognizable in commercial vehicles.



**Figure 2.** Speed-torque variation of the highway engine [10]

In terms of the characteristics of suburban/rural traffic, it is somewhere between urban and highway traffic. The place where the main road network typically passes is twice with single-lane roads. Intersections are rare, but they are flat and affect traffic. The fleet's composition is mixed, because in addition to the vehicles on the highway, agricultural vehicles and bicycles also travel on certain road sections. Longitudinal vehicle dynamics vary more than on the highway, but the average speed is closer to the highway (75 km/h, [12]). Lateral vehicle dynamics are similar to highway use [17].

Table 1.	Summary of existing road mobility form
	characteristics

Criteria	Urban	Rural	Motorway
Nr. of par-	1-4	1	2+
alel lines			
Se-	none	none	physical
pearation			separation
of lines			
Crossing	all possi-	limited	no same
types	ble types		level cross-
			ing
Nr. of	high	moder-	no (sepa-
crossings		ate	rate lines)
Average	under 30	app. 75	app. 110
speed	km/h	km/h	km/h
Minimum	no	no	70 km/h
speed			
Longitud-	turbulent	moder-	simple
nal vehicle		ate	
dynamics			
Lateral ve-	turbulent	simple	simple
hicle dy-			
namics			
Interaction	very high	moder-	low
numbers		ate	
between			
parctic-			
ipants			
Homogen-	inhomo-	moder-	homoge-
ity of par-	gen	ate	nous
ticipants			
Vehicle	turbulent	moder-	stable
technology		ate	
effects			

### III. MEASURING VEHICLE BEHAVIOUR

Emissions from road mobility account for a large share of pollutant and carbon dioxide emissions. The European Environment Agency's 2018 air quality report [18] confirms that air pollution is the main environmental health risk. Road transport is responsible for 39% of nitrogen oxide emissions, 28% of particulate emissions and 20% of carbon monoxide emissions. For this reason, road vehicles placed on the EU market since 1970 are subject to type approval, which has been part of the Euro 1 standard since its introduction in 1992. Currently, the active pollution control standard applies to passenger cars from Euro 6d onwards [19].

As a result, road transport has reduced its emission rate since 1990. However, the continued growth of the EU fleet and in particular, the increasing share of diesel vehicles (which traditionally have higher  $NO_x$  and PM emissions than petrol vehicles) have reduced the scope for improving air quality. Note that recent studies have confirmed the critical aspects of old diesel vehicles (Euro 0 to Euro 3) but have reduced the impact of modern diesel compared to modern petrol

vehicles, at least to the extent that this applies to particulates. In addition, the deviations between expected and actual pollutant reductions also increased due to the emission differences between the vehicles tested in the laboratory and on the road. With different rolling resistance and aerodynamic drag, free gear shift strategy and driving style, non-zero positive altitude gain and unregulated environmental conditions, emissions on the road are expected to vary compared to those in controlled vehicles—laboratory experiment following the prescribed speed curve. In 2007, the JRC started a series of experimental activities to investigate real-world emissions using on-board instruments such as PEMS. In particular, for light commercial vehicles (i.e. passenger cars), large differences between laboratory and road vehicles were found in terms of NO<sub>x</sub> emissions from diesel cars [20]. These findings and other elements led to regulatory efforts: In 2016, the EU adopted the first RDE package [21], establishing procedures, equipment requirements and assessment. Since then, RDE has undergone three major legislative changes. A non-exhaustive chronology of the EU RDE legislation is presented in Table 2, which includes the relevant JRC reports. Currently, the 4th RDE legislative package [22] is active and valid for Euro 6d-TEMP vehicles from January 2019.

The main scientific link between road mobility splitting and transport sustainability is vehicle emissions testing. Since the three categories presented described most of the vehicle use in the last century, the test methods were developed for them [23].

During the tests, the qualification tracks consist of three separable sections: highway, urban and mixed, which map the previously presented categories. Figure 3 shows that the test sections' characteristics are separated in terms of acceleration\*speed indication and acceleration while driving. The results of the tests are used in many places, for example in the emission assessment of new vehicles or in the determination of catalog consumption.

The data set was characterized by a speed in the city of  $\approx 30$  km/h, a speed in the countryside of  $\approx 75$  km/h and a speed on the highway of  $\approx 110$  km/h.

### IV. CURRENT DATA ON URBAN MOBILITY

According to the survey, most people still travel by car on their daily journeys: 45 percent mainly use their private car, 23 percent use public transport, 16 percent use a micro-mobility device and 14 percent reach their destination on foot. According to previous data, 16 percent of the Hungarian population cycles on weekdays, and four thousand designated cycle paths now serve this purpose. The data also show that micromobility in Hungary is mainly used for shorter distances: 60 percent of electric scooter riders and 50 percent of cyclists travel less than five kilometres per trip; the accident rate of e-scooters is

three times higher than that of cyclists. According to the survey, many people see cycling in traffic as a stress factor. At the same time, other new means of transport have recently emerged as part of the mobility transition: electric bicycles, Segways and electric scooters. These vehicles already participate in traffic every day, but on public roads they often appear in disorderly conditions [24].

The long-term mobility visions also point in a similar direction. On the one hand, individual transport in cities, especially in traffic-calmed zones, will be pointless due to the strengthening of alternatives such as micromobility, bicycle, walking, and on the other hand, the increase in the price of new vehicles will not make sense, so it is possible to own them [25]. The car-free inner cities with few parking spaces being introduced in more cities will also facilitate this [26].

### V. RESULTS

The changing road mobility is less and less described by the triple use of city-country-road-highway, which has been well suited until now, because urbanization has reached such a level that a new area of use has emerged: the city center.

Its peculiarity is that it is located in metropolises and in many cases is identical to the historic city center. The existing road network is not suitable for the transit function it will take on once the residents have moved out, so from a car traffic perspective it can be characterized as a traffic-calmed or closed area. In these areas, the use value of private cars is reduced due to restrictions on pollution classification or powertrain and the limited number of parking spaces. At a system level, the objective is to reduce emissions. This can be achieved by prioritizing public transport, even public transport with fixed tracks, footpaths and - in many cases shared - micromobility devices. Vehicle dynamics can only be interpreted for the remaining vehicles in these areas. There is a lot of interaction with pedestrians, typically the speed is low, averaging 10 km/h. The further development of cognitive mobility significantly influences inner-city mobility, the participants are equipped with sensors, location sensors and occupancy sensors, thus promoting highly efficient mobility through networking with the help of mobile devices.

The introduction of the new form of use opens up new scope, especially for urban mobility planning, and opens up the possibility of using economic means to contribute to the most sustainable mobility possible. The new category is in symbiosis with the other categories, since the difference does not consist of a unit jump at the interfaces, but in a fuzzy system. The solutions observed here are partially and spatially to a lesser extent shifted to the surrounding areas.

**Table 2.** Proposal for the introduction of a new

mode of transport

mode of transport							
Crite-	Down-	Urban	Rural	Motor-			
ria	town			way			
Nr. of	1/none	1-4	1	2+			
parallel							
lines							
Separa-	none	none	none	physical			
tion of				separa-			
lines				tion			
Cross-	merg-	all	lim-	no same			
ing	ing	possi-	ited	level			
types		ble		crossing			
• • •		types					
Nr of	very	high	mod-	no (sep-			
cross-	high		erate	arate			
ings	8			lines)			
Aver-	app. 10	under	app.	app. 110			
age	km/h	30	75	km/h			
speed	1111,11	km/h	km/h	1111/11			
Mini-	no	no	no	70 km/h			
mum	(walk-	110	110	/ U KIII/II			
speed	ing)						
Longi-	limited	turbu-	mod-	simple			
tudnal	by the	lent	erate	simple			
vehicle	-	iciit	Crate				
	speed						
dynam-							
ics	.1	4 .1.	1 .	1 .			
Lateral	dy-	turbu-	simple	simple			
vehicle	namic	lent					
dynam-							
ics							
Interac-	very	very	mod-	low			
tion	high,	high	erate				
num-	pedes-						
bers be-	trians						
tween							
parctic-							
ipants							
Но-	moder-	inho-	mod-	ho-			
mogen-	ate	mogen	erate	mogen-			
ity of				ious			
partici-							
pants							
Vehicle	to be	turbu-	mod-	stable			
tech-	deter-	lent	erate				
nology	mined						
effects							
Energy	very	high	mod-	very			
con-	low	_	erate	high			
sump-	(tbd)			-			
tion per							
partici-							
pants							
Emis-	very	very	mod-	high			
sion per	low	high	erate	<i>5</i>			
partici-	(tdb)	8	110				
parties	(100)						
Pants		l	l				

### VI. CONCLUSION

The social music of the 21st century and one of its main pillars, mobility, is changing thanks to the accelerated technological development. The criteria by which we have characterized mobility so far may need to be revised. In our work, we study the urban-rural-highway-based separation, which is widespread and crucial from the perspective of sustainability assessment of road mobility devices. We present its characteristics and consider the testing procedures based on them. By comparing these with the mobility trends, we point out the need to complement them and propose the introduction of a new category, indicating its main dimensions and highlighting the areas where further research is needed.

### VII. ACKNOWLEDGEMENT

The project presented in this article is supported by OTKA 2021/138053.

### REFERENCES

- [1] Federal Highway Administration, *Urban/Rural Split of Travel*. Available: <a href="https://www.fhwa.dot.gov">https://www.fhwa.dot.gov</a>. Accessed: 2024-09-01.
- [2] A. Zardini and P. Bonnel, "Real Driving Emissions Regulation: European Methodology to Fine Tune the EU Real Driving Emissions Data Evaluation Method," EUR 30123 EN, Publications Office of the European Union, Luxembourg, 2020. ISBN 978-92-76-17157-7. https://doi.org/10.2760/176284
- [3] T. Fleischer, "Harmonious coexistence of urban activity and flow spaces," in *Proceedings of the 10th European Transport Congress: New Paths in Urban and Intercity Transport*, J. Tóth, Ed. Budapest: Közlekedéstudományi Egyesület European Platform of Transport Sciences, 2012, pp. 44–48.
- [4] K. P. De-Toledo, S. O'Hern, and S. Koppel, "A city-level transport vision for 2050: Reimagined since COVID-19," *Transport Policy*, vol. 132, pp. 144–153, 2023. <a href="https://doi.org/10.1016/j.tranpol.2022.12.022">https://doi.org/10.1016/j.tranpol.2022.12.022</a>
- [5] H. A. Al-jameel and A. Jihad, "Some Traffic Characteristics of Rural Roads in Iraq," in *Cur*rent Approaches in Science and Technology Research, vol. 6, 2021. <a href="https://doi.org/10.9734/bpi/castr/v6/9705D">https://doi.org/10.9734/bpi/castr/v6/9705D</a>
- [6] G. Zsigmond, "Közlekedés térben és időben [Transportation in Space and Time]," *Városi Közlekedés*, 2nd online issue, 2021. Available: <a href="https://www.acade-mia.edu/44814067/K%C3%B6zle-ked%C3%A9s">https://www.acade-mia.edu/44814067/K%C3%B6zle-ked%C3%A9s</a> t%C3%A9rben %C3%A9s id %C5%91ben. Accessed: 2024-09-01.

### **AUTHOR CONTRIBUTIONS**

**M. Zöldy**: Conceptualization, Experiments, Theoretical analysis, Writing, Review and editing.

### DISCLOSURE STATEMENT

The author declare that he has no known competing financial interests or personal relationships that could have appeared to influence the work reported in this paper.

### **ORCID**

M. Zöldy http://orcid.org/0000-0003-1271-840X

- [7] M. Zöldy, "Improving heavy duty vehicles fuel consumption with density and friction modifier," *International Journal of Automotive Technology*, vol. 20, pp. 971–978, 2019. https://doi.org/10.1007/s12239-019-0091-y
- [8] M. Zoldy, M. S. Csete, P. P. Kolozsi, P. Bordas, and A. Torok, "Cognitive sustainability," *Cognitive Sustainability*, vol. 1, no. 1, 2022. https://doi.org/10.55343/cogsust.7
- [9] L. Filina-Dawidowicz, S. Stankiewicz, K. Čižiūnienė, and J. Matijošius, "Factors influencing intermodal transport efficiency and sustainability," *Cognitive Sustainability*, vol. 1, no. 1, 2022. <a href="https://doi.org/10.55343/cogsust.9">https://doi.org/10.55343/cogsust.9</a>
- [10] A. Boldizsár, F. Mészáros, and E. Torok, "Social and economic analysis of the EU road freight transport fleet," *Cognitive Sustainability*, vol. 1, no. 2, 2022. <a href="https://doi.org/10.55343/cogsust.16">https://doi.org/10.55343/cogsust.16</a>
- [11] A. Vučetić, V. Sraga, B. Bućan, K. Ormuž, G. Šagi, P. Ilinčić, and Z. Lulić, "Real Driving Emission from Vehicle Fuelled by Petrol and Liquefied Petroleum Gas (LPG)," *Cognitive Sustainability*, vol. 1, no. 4, 2022. https://doi.org/10.55343/cogsust.38
- [12] T. Koller, C. Tóth-Nagy, and J. Perger, "Implementation of vehicle simulation model in a modern dynamometer test environment," *Cognitive Sustainability*, vol. 1, no. 4, 2022. https://doi.org/10.55343/cogsust.29
- [13] Á. Nyerges and M. Zöldy, "Hosszirányú járműmodell fejlesztése elektromos járművek hatótáv becslésére [Longitudinal vehicle model development for range estimation in electric vehicles]," Műszaki Szemle, vol. 74, 2020.

- Available: <a href="https://ojs.emt.ro/muszaki-szemle/article/download/258/165">https://ojs.emt.ro/muszaki-szemle/article/download/258/165</a>. Accessed: 2024-09-01.
- [14] M. Zöldy, A. Holló, and A. Thernesz, "Development of More Efficient Fuels for Niche Markets," in *Proceedings of the FISITA 2012: Advanced Internal Combustion Engines*. Available: <a href="https://www.researchgate.net/publication/282764062">https://www.researchgate.net/publication/282764062</a> Development of More Efficient Fuels for Niche Markets. Accessed: 2024-09-01.
- [15] T. Péter, F. Szauter, Z. Rózsás, and I. Lakatos, "Integrated application of network traffic and intelligent driver models in the test laboratory analysis of autonomous vehicles and electric vehicles," *International Journal of Heavy Vehicle Systems*, vol. 27, no. 1–2, pp. 227–245, 2020. <a href="https://doi.org/10.1504/IJ-HVS.2020.104422">https://doi.org/10.1504/IJ-HVS.2020.104422</a>
- [16] V. Jóvér, Z. Major, A. Németh, D. Kurhan, M. Sysyn, and S. Fischer, "Investigation of 'Open' Superstructure Tramway Tracks in Budapest," *Infrastructures*, vol. 8, no. 2, 2023. https://doi.org/10.3390/infrastructures8020033
- [17] S. Kocsis Szürke, G. Kovács, M. Sysyn, J. Liu, and S. Fischer, "Numerical Optimization of Battery Heat Management of Electric Vehicles," *Journal of Applied and Computational Mechanics*, vol. 9, no. 4, pp. 1076–1092, 2023. https://doi.org/10.22055/jacm.2023.43703.411

- [18] T. Péter, I. Lakatos, F. Szauter, and D. Pup, "Complex analysis of vehicle and environment dynamics," in 2016 12th IEEE/ASME International Conference on Mechatronic and Embedded Systems and Applications (MESA), IEEE, 2016, pp. 1–7. https://doi.org/10.1109/MESA.2016.7587112
- [19] T. Fleischer, "The sustainability issues of mobility services: social impacts, spatial and temporal management," *Közlekedéstudományi Szemle*, vol. 69, no. 1, pp. 49–57, 2019.
- [20] T. Fleischer, "Some questions on the development of the Hungarian expressway network," *Közlekedéstudományi Szemle*, vol. 44, no. 1, pp. 7–24, 1994.
- [21] M. Zöldy, P. Baranyi, and Á. Török, "Trends in Cognitive Mobility in 2022," *Acta Polytechnica Hungarica*, vol. 21, pp. 189–202, 2024. https://doi.org/10.12700/APH.21.7.2024.7.11
- [22] K. Bebkiewicz, Z. Chłopek, H. Sar, and M. Zi-makowska-Laskowska, "Assessment of the impact of vehicle traffic conditions: urban, rural, and highway, on the results of pollutant emissions inventory," *Archives of Transport*, vol. 60, no. 4, pp. 57–69, 2021. https://doi.org/10.5604/01.3001.0015.5477



This article is an open access article distributed under the terms and conditions of the Creative Commons Attribution NonCommercial (CC BY-NC 4.0) license.

### ACTA TECHNICA JAURINENSIS



Vol. 17, No. 4, pp. 169-176, 2024 10.14513/actatechjaur.00752



Research Article

## Design of hydraulic lift system of technical equipment working in amusement industry

Miroslav Blatnický<sup>1</sup>, Ján Dižo<sup>1,\*</sup>, Alyona Lovska<sup>1</sup>, Vadym Ishchuk<sup>1</sup>

<sup>1</sup>Department of Transport and Handling Machines, University of Žilina Univerzitná 8215/1, 010 26 Žilina, Slovak Republic \*e-mail: jan.dizo@fstroj.uniza.sk

Abstract:

This paper examines the design and application of a telescopic hydraulic system for amusement industry equipment that experiences cyclic passenger loads. The system comprises three hydraulic cylinders, each with different diameters, which activate at various points as the device moves. To achieve static balance and lift the main beam from a horizontal to a vertical position, the forces exerted by the cylinders were calculated using static equilibrium equations. The system's design, including the length and angle of each cylinder, was based on the technical specifications of the equipment. Analytical and numerical methods were used to ensure the correct sizing of the cylinders and the system's overall effectiveness, resulting in a structure that operates safely and efficiently.

Keywords: Structural design; Technical device; Calculation; Analysis

### I. Introduction

Nowadays, more than ever, it is noticeable that work comes first in life. Sadly, there is no time left for ordinary joy in life, so people should diversify their free time [1]. Relaxing from everyday worries is important in preventing psychological and physical problems brought about by such a hectic lifestyle [2-4]. Therefore, the contribution of the amusement industry and its technical facilities should not be negligible [5].

The historical development of technology used in the entertainment industry was analyzed in detail in works [1, 6], which was followed up in work [7], where the authors, among other things, also addressed the materials used in the construction of such devices [8-11], the design of the drive and units of the proposed device in question (**Fig. 1** to **Fig. 4**), carrying passengers, were presented.

Normative requirements that must be met in the design of technical equipment working in the amusement industry within the Slovak Republic were published in papers [12, 13]. In them, the proposed device was presented with geometry and individual structural units such as seats for passengers, gondolas carrying the seats, lattice structures carrying the gondolas, a drive mechanism,

the main beam of the device and the movement possibilities of the proposed device. Structural proposals were supported by strength analytical and numerical calculations. The presented issue is a large-scale issue; therefore, the other two works [14, 15] were aimed at the research, design and calculation of other structural units of the device. The current work provides the results in a design of hydraulic cylinders used for positioning the given technical equipment [16-18]. The considered movement possibilities of the lifting mechanism are shown in **Fig. 3** and **Fig. 4**.



Figure 1. A three-dimensional CAD model of the structural design of the technical device working in the amusement industry – Position No. 1

Position No. 1 of the proposed device (Fig. 1) represents the rest state when the device is prepared

for the boarding and exit of passengers to individual gondolas. As it was published in previous works, the gondola is designed for two passengers with a human weight of 100 kg (the gondola load safety coefficient required by the standard is 6) with a minimum required height of 135 cm (follows from the standard STN EN 547-3 + A1 due to safety of the mechanism). The number of gondolas is 18, representing 36 seated passengers spread over a wheel spacing of 5.73 m.

Position No. 2 of the proposed device (**Fig. 2**) represents the tilting of the gondolas in the direction of the acting centrifugal force, which is created by the effect of rotating the wheel at the proposed revolutions 14 min<sup>-1</sup>, which will cause a maximum gravity acceleration of 2.2 g the passengers will feel. According to the STN EN 13814 standard, maximum of 6 g is allowed. The structure is rotated by an electric motor using a gear. More information about the designed device's operation principle can be found in the works [4-7].



Figure 2. A three-dimensional CAD model of the structural design of the technical device working in the amusement industry – Position No. 2



Figure 3. A three-dimensional CAD model of the structural design of the technical device working in the amusement industry – Position No. 3

Position No. 3 of the proposed device (**Fig. 3**) represents the engagement of the lifting mechanism in operation when the wheel with gondolas is raised using a hydraulic cylinder, i.e., from a horizontal position (**Fig. 2**) to a vertical one (**Fig. 4**). Here, the

main component is the beam, whose load, geometry and principle of operation were solved by the authors in the paper [8].

The main beam will be raised using a hydraulic system with a telescopic cylinder, while the geometry of the mechanism resulted in the lengths of the cylinders  $l_{v1} = 1.4$  m,  $l_{v2} = 1.6$  m,  $l_{v3} = 1.8$  m and the total length of extension from the point of attachment of the cylinders will be  $l_{vc} = 6.96$  m. The CATIA V5 software was used to determine the angles at which the cylinders would push into the beam.



Figure 4. A three-dimensional CAD model of the structural design of the technical device working in the amusement industry – Position No. 4

### II. DETERMINATION OF THE NECESSARY LIFTING FORCES OF HYDRAULIC CYLINDERS

The cylinder No. 1 starts to push the structure at the angle of  $\alpha_1 = 50^{\circ}$  (**Fig. 5**). In the given figure, point 1 indicates the attachment point of the telescopic system in the anchoring of the device, the thick lines are the intended beam (length from the rotary link to the holder of the telescopic system), the dashed lines depict the length of the cylinders' extension, before the start of pushing to the final position of the device. The values  $\alpha_1 = 50^{\circ}$ ,  $\alpha_2 =$  $46.88^{\circ}$ ,  $\alpha_3 = 53.484^{\circ}$  and  $\alpha_4 = 67.689^{\circ}$  are the angles at which the telescopic system pushes at different positions of the beam,  $\beta_1 = 23.301^{\circ}$  and  $\beta_2 = 51.032^{\circ}$ are the angles at which the device lifts. In previous publications, the values of  $F_k = 304,210.65 \text{ N}$  (load from the weight of the wheel structure) and  $F_m =$ 16,196.31 N (load from the weight of the electric motor with accessories used to rotate the wheel with nacelles) were determined. Thus, to determine the force exerted by the cylinders, adding the beam  $F_n$ itself is necessary, which can be written as a continuous load  $q_n$  (see Eqs. (1-2)). This load can be

obtained according to Eq. (2) if the mass of the beam  $m_n = 10,058.57$  kg (Eq. (1)) and the height of the beam section h = 1.3 m are known:

$$F_n = m_n \cdot g , \qquad (1)$$

 $F_n = 10,058.57 \cdot 9.81 = 98,674.57 \text{ N},$ 

$$q = \frac{F_n}{h} \,, \tag{2}$$

$$q = \frac{98,647.57}{1.3} = 75,903.52 \text{ N} \cdot \text{m}^{-1}$$
.

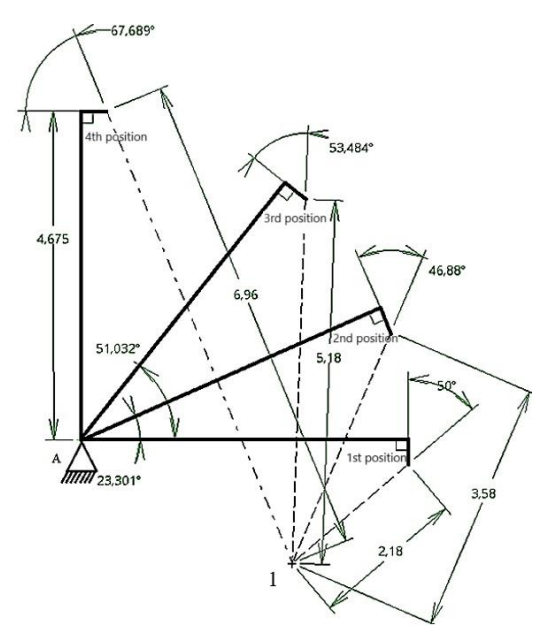
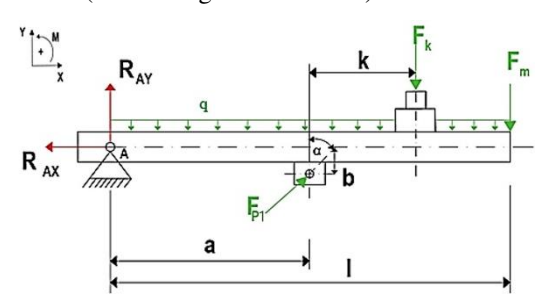


Figure 5. A designed geometry of the extrusion of individual cylinders

Length dimensions of the beam according to **Fig. 6** are a = 4.675 m (a distance from a rotary coupling to a cylinder attachment), b = 0.375 m (a distance from a beam axis to a horizontal axis of a cylinder attachment), k = 3.325 m (a distance from a wheel axis to a hydraulic cylinder attachment axis), l = 8.566 m (a total length of the beam).



**Figure 6.** A calculation scheme of the hydraulic cylinder No. 1 – the 1<sup>st</sup> position

The initial force acting from the hydraulic cylinder No. 1 can be expressed using Eq. (3):

$$\sum_{i} M_{iA} = 0 \implies$$

$$F_{P1} \cdot \cos \alpha \cdot a + F_{P1} \cdot \sin \alpha \cdot b -$$

$$-F_{m} \cdot l - F_{k} \cdot (k+a) - \frac{q \cdot l^{2}}{2} = 0.$$
(3)

The angle  $\alpha = 50^{\circ}$  applies for the cylinder No. 1 needed to generate the force of the first cylinder. Then, it is get (Eq. (4)):

$$F_{P1} = \frac{F_m \cdot l + F_k \cdot (k+a) + \frac{q \cdot l^2}{2}}{\cos \alpha \cdot a + \sin \alpha \cdot b}$$
(4)

and after substituting, we get  $F_{P1}$  = = 1,627,186.68 N.

The obtained force is considered only at the beginning of the first cylinder pushing. Logically, further forces must decrease until the final position of the stroke. When cylinder No. 1 extends by 1.4 m, the telescopic system starts to push out the second cylinder. According to **Fig. 7**, the action of the forces against the beam changes due to lifting; therefore, it is necessary to construct another balance equation when the beam is no longer in a horizontal position. To begin with, the calculation can be simplified by choosing a local coordinate system.

There are considered the obtained force only at the beginning of pushing the cylinder No. 1. Logically, further forces must decrease until the final position of the stroke. When cylinder No. 1 extends by 1.4 m, the telescopic system starts to push out the cylinder No. 2. It can be seen, according to **Fig. 7**, that the action of the forces against the beam changes due to lifting; therefore, it is necessary to construct another equation of equilibrium, when the beam is no longer in a horizontal position. To begin with, the calculation can be simplified by choosing a local coordinate system.

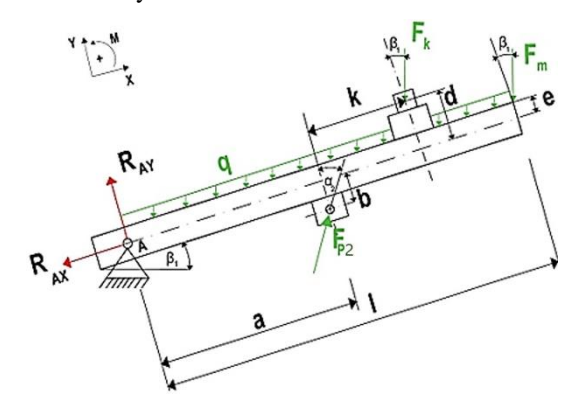


**Figure 7.** A calculation scheme of the hydraulic cylinder No. 2 – the  $2^{nd}$  position

The angle, by which the beam is lifted, will be  $\beta_1$  = 23.301° and the angle at which the second cylinder pushes will be  $\alpha_2$  = 46.88°. Since the forces  $F_k$  and  $F_m$  are not normal to the axis of the beam, the forces

for the x axis must also be considered. The center of gravity, to which the force  $F_m$  acts, is distance from the main axis of the beam marked as e and it has a value of e = 0.125 m, and the distance d = 1.171 m applies to the force  $F_k$ . Then, according to **Fig. 7**, it is possible to compile the moment equation to the point A for which applies (Eq. (5)):

$$\sum_{i} M_{iA} = 0 \implies -\frac{q \cdot l^{2}}{2} \cdot \cos \beta_{1} - F_{m} \cdot \left[\cos \beta_{1} \cdot l - \sin \beta_{1} \cdot e\right] - F_{k} \cdot \left[\cos \beta_{1} \cdot (a + k) - \sin \beta_{1} \cdot d\right] + F_{p} \cdot \left[\cos \alpha_{2} \cdot a + \sin \alpha_{2} \cdot b\right] = 0.$$
(5)

The force for the hydraulic cylinder No. 2 is possible to get by a modification of Eq. (5), (see Eq. (6)):

$$F_{P2} = \frac{F_m \cdot \cos \beta_1 \cdot l}{\cos \alpha_2 \cdot a + \sin \alpha_2 \cdot b} - \frac{F_m \cdot \sin \beta_1 \cdot e + F_k \cdot \cos \beta_1 \cdot (a+k)}{\cos \alpha_2 \cdot a + \sin \alpha_2 \cdot b} - \frac{F_k \cdot \sin \beta_1 \cdot d + \frac{q \cdot l^2}{2} \cdot \cos \beta_1}{\cos \alpha_2 \cdot a + \sin \alpha_2 \cdot b}.$$
(6)

and after substituting, it will be  $F_{P2} = 1,377,410.81$  N.

The initial force for the cylinder No. 3 can be expressed similarly to the cylinder No. 2 according to Eq. (5) because only the angles at which the forces act will change (**Fig. 8**). The values of the angles are  $\beta_2 = 51.032^{\circ}$  and  $\alpha_3 = 53.484^{\circ}$ :

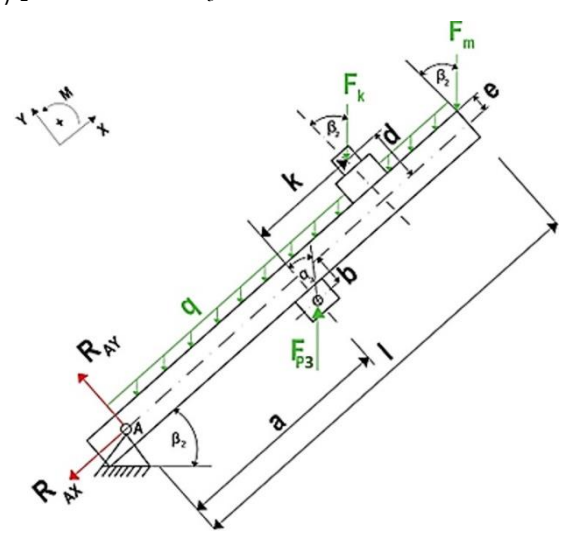


**Figure 8.** A calculation scheme of the hydraulic cylinder No. 3 – the 3<sup>rd</sup> position

Then, the force for the cylinder No. 3 will be given in Eq. (7):

$$F_{P3} = \frac{F_m \cdot \cos \beta_1 \cdot l}{\cos \alpha_3 \cdot a + \sin \alpha_3 \cdot b} - \frac{F_m \cdot \sin \beta_2 \cdot e + F_k \cdot \cos \beta_2 \cdot (a+k)}{\cos \alpha_3 \cdot a + \sin \alpha_3 \cdot b} - \frac{F_k \cdot \sin \beta_2 \cdot d + \frac{q \cdot l^2}{2} \cdot \cos \beta_2}{\cos \alpha_3 \cdot a + \sin \alpha_3 \cdot b}$$

$$(7)$$

and after substituting  $F_{P3} = 1,002,363.57$  N.

After determining all three initial forces, it is clear that the force with which the telescopic system needs to be pushed on the beam decreases. The beam tilting helps to it. This means there is a certain dependence between the force required to lift the beam and the length of extension of the cylinders. This dependence can be written down graphically. However, firstly, it is necessary to determine the final force from the cylinders so that the dependence can be shown throughout the stroke. The forces acting on the device in the vertical position are, therefore, according to **Fig. 9**, where the force from the cylinders acts at an angle  $\alpha_4 = 67.689^{\circ}$ . It is possible to set, based on **Fig. 9**, the moment equation to point A, for which it is valid (see Eq. (8)):

$$\sum_{i} M_{iA} = 0 \implies F_{m} \cdot e + F_{k} \cdot d + F_{p_{4}} \cdot \cos \alpha_{4} \cdot a + F_{p_{4}} \cdot \sin \alpha_{4} \cdot b = 0.$$
(8)

Modification and substituting lead to the force from the telescopic cylinders in the vertical position of the amusement device  $F_{P4} = -168,851.77$  N.

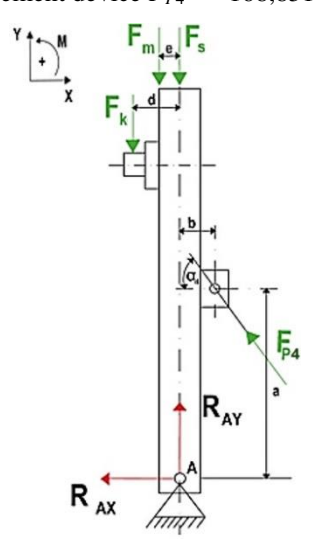


**Figure 9.** A calculation scheme for the vertical position – the 4<sup>th</sup> position

The force for the vertical position of the amusement device came out in the negative direction, because the forces  $F_m$  and  $F_k$  are located behind the pivot point of the beam. Thus, at a certain

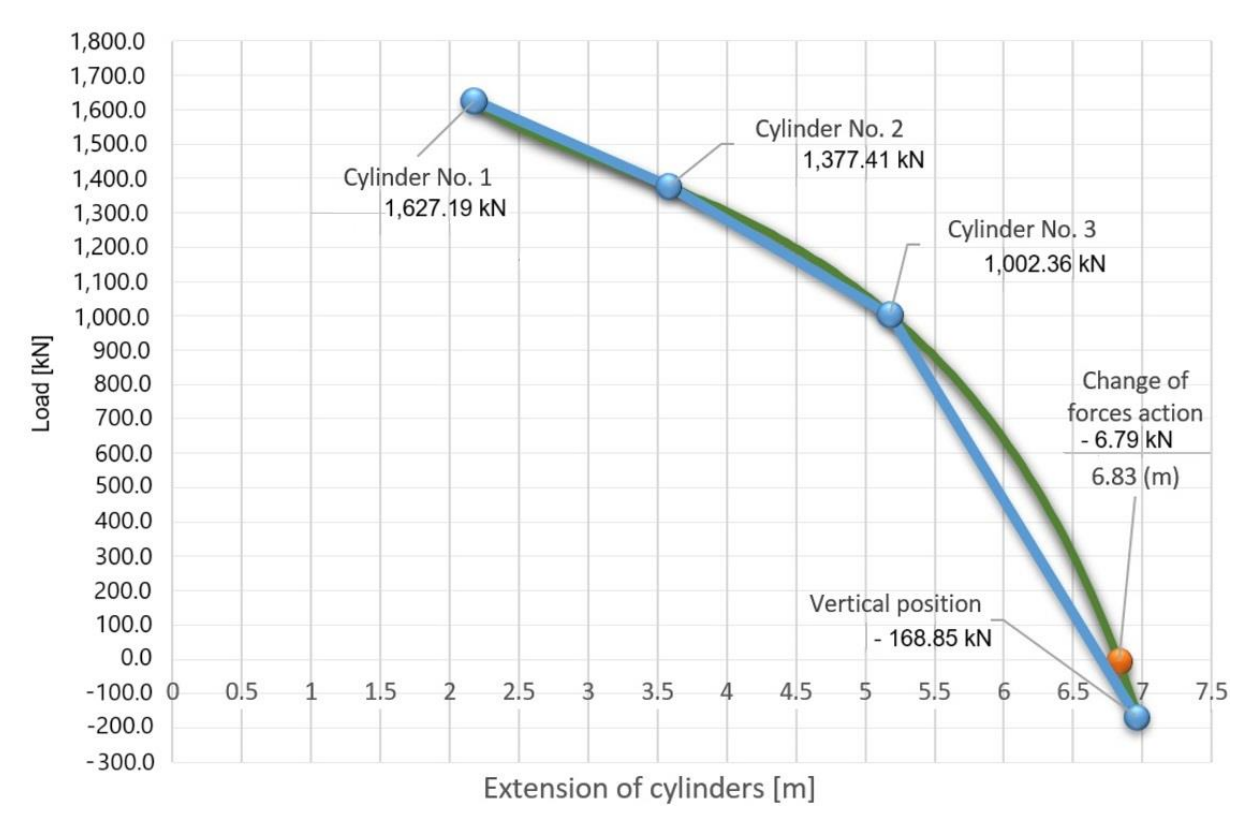


Figure 10. A dependence of the load on the extension of cylinders

point of tilt, these forces stop creating a moment against the  $F_{PIEST\,4}$  force, but they begin to support this force and help it rotate the device around the rotational coupling. Then, the load's dependence on the cylinders' extension is shown in **Fig. 10**.

The first, a blue curve, is created from 4 points connected by linear lines, which means the curve considers only the cylinders' initial forces in the places where they start to push to the final value. The second curve, shown by a green curve, represents the function processed using the relation (6), where the results of the forces were graduated by 5 cm and thus 97 results were processed, from which a more accurate hyperbolic function is obtained. According to these results, it can be concluded that the proposed device reaches beyond the axis of rotation approximately at a length of 6.8 m measured from the mount of the telescopic system.

### III.DESIGN OF THE CYLINDER DIAMETERS ACCORDING TO THE INITIAL FORCES

The correct diameters of the cylinders of the telescopic system must be determined to lift the proposed technical device safely. These diameters can be quantified using simple relationships when the initial cylinder lift force and feed fluid pressure are known. The pressure in the system will be set to p = 35 MPa. Therefore, Eq. (9) is valid for the cylinder No. 1:

$$F_{P1} = p \cdot S_1 \implies S_1 = \frac{F_{P1}}{P}$$
  
 $S_1 = \frac{1,627,186.68}{35} = 46,491.02 \text{ mm}^2.$  (9)

Then, the radius of the cylinder No. 1  $r_1$  is (see Eq. (10)):

$$S_1 = \pi \cdot r_1^2 \implies r_1 = \sqrt{\frac{S_1}{\pi}}$$

$$r_1 = \sqrt{\frac{46,491.05}{\pi}} = 121.65 \text{ mm}$$
(10)

at which, the active diameter of the hydraulic cylinder  $D_1$  is given by Eq. (11):

$$D_1 = 2 \cdot r_1 = 2 \cdot 121.65 = 243.3 \text{ mm}$$
 (11)

A normalized cylinder with the diameter  $D_1 = 245$  mm was chosen. Similarly, it is possible to determine the diameter of the cylinder No. 2  $D_2$  using Eqs. (12-14):

$$F_{P2} = p \cdot S_2 \implies S_2 = \frac{F_{P2}}{P}$$
  
 $S_2 = \frac{1,337,410.81}{35} = 39,354.59 \text{ mm}^2.$  (12)

The radius of the cylinder No. 2  $r_2$  is (see Eq. (13)):

$$S_2 = \pi \cdot r_2^2 \implies r_2 = \sqrt{\frac{S_2}{\pi}}$$

$$r_2 = \sqrt{\frac{39,354.59}{\pi}} = 111.92 \text{ mm}$$
(13)

at which, the active diameter of the hydraulic cylinder No. 2 is given by Eq. (14):

$$D_2 = 2 \cdot r_2 = 2 \cdot 111.92 = 223.84 \text{ mm},$$
 (14)

therefore, the normalized cylinder with the diameter  $D_2 = 245$  mm was chosen.

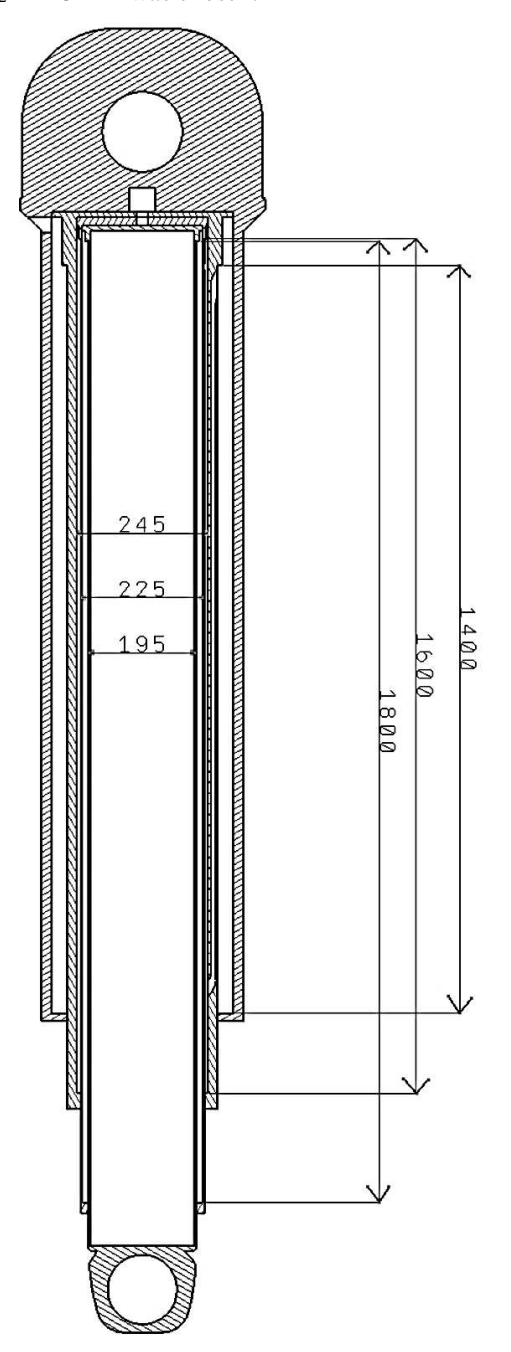


Figure 11. The main dimensions of the designed telescopic system

Finally, Eqs. (15-17) serve to calculate the diameter of the cylinder No. 3:

$$F_{P3} = p \cdot S_3 \implies S_3 = \frac{F_{P3}}{P}$$
  
 $S_3 = \frac{1,002,363.57}{35} = 28,638.96 \text{ mm}^2.$  (15)

The radius of the cylinder No. 3 is (see Eq. (16)):

$$S_3 = \pi \cdot r_3^2 \implies r_3 = \sqrt{\frac{S_3}{\pi}}$$

$$r_3 = \sqrt{\frac{28,638.96}{\pi}} = 95.48 \text{ mm}$$
(16)

and the active diameter of the hydraulic cylinder No. 3 is given by Eq. (17):

$$D_3 = 2 \cdot r_3 = 2 \cdot 95.48 = 190.96 \text{ mm}$$
 (17)

Based on the previous calculation, the normalized diameter of the hydraulic cylinder No. 3 is chosen with the diameter of  $D_3 = 195$  mm. According to the observed diameters of individual hydraulic cylinders, it is possible to set up a telescopic system with corresponding diameters, as depicted in **Fig. 11**.

### IV. CONCLUSION

The paper discussed the research on a structural of a telescopic hydraulic implementable in a technical equipment cyclically stressed by the variable load from passengers. Overall, many publications on this issue focused on normative analytical and numerical solution methods. The beginning of the research consisted of the analysis of the historical development of the entertainment industry from the beginning to the present day, together with the presentation of the main components used in constructing such facilities and their material base. Here, information resulting from valid procedures and standards such as STN EN 13814 and STN EN 13814-1 was fully utilized. In the following solution to the problem, the proposed type of amusement device was presented together with the technical specifications and the place of an implementation, where the maximum number of passengers was 18 and other parameters of the device were normatively derived accordingly. The research was further devoted to creating a 3D CAD model with the help of the CATIA V5 software , which was logically based on derived dimensional calculations. After designing the geometry of the individual components, analytical and numerical methods were used to accurately design the selected structural units as a gondola assembled for two passengers and adapted to the main dimensions of the body according to the STN EN 547-3 + A1 standard, with the maximum load capacity of 100 kg per passenger. Further calculations focused on the design of the truss structure and the hollow shaft,

verified using analytical and numerical methods. During the design, attention was also paid to the specific calculation of the electric motor's power, which resulted in an electric motor with a conicalfrontal gearbox with an output of 90 kW, together with the gear transmission design. The main beam of the amusement device was checked for the required deflection according to the STN EN 13814 standard using analytical calculations, and the numerical method was also checked in the ANSYS software. All these steps resulted in the presented work in the possibility of determining the dependence of the load on the extension of the cylinders of the telescopic system, and a suitable diameter of the individual cylinders was proposed. This system will consist of three hydraulic cylinders with different diameters, and each cylinder starts pressure at a different device position. However, this was preceded by quantifying the forces with which the cylinders will act on the main beam to achieve static equilibrium and lift it to the desired position (from horizontal to vertical). This, the forces were determined using the static equilibrium equations. The geometry of the cylinders (length, angles at which the cylinders begin to act on the beam) was chosen based on the parameters of the proposed technical device resulting from previously published research work.

### ACKNOWLEDGEMENT

This publication was supported by the Cultural and Educational Grant Agency of the Ministry of Education of the Slovak Republic in the project KEGA 031ŽU-4/2023: Development of key competencies of the graduate of the study program Vehicles and Engines.

### REFERENCES

- [1] M. Blatnický, J. Dižo, D. Molnár, Overview of historical development and analysis of the current state of transport and handling machines in the entertainment industry (In Slovak), Technológ (14) (2) (2022) pp. 61-64.
- [2] R. Zbončák, J. Ondrášek, Stress Analysis of the Hybrid 'Steel-Composite' Disc in a Carousel Body of an Indexing Gearbox Turret Follower, 5th International Conference of IFToMM Italy, IFIT 2024, Turin, Mechanisms and Machine Science, pp. 126-133. https://doi.org/10.1007/978-3-031-64553-2\_15
- [3] P. Koščák, Ľ. Ambriško, K. Semerád, D. Marasová, jr., V. Mitrík, Numerical and Experimental Stress-Strain Analysis of a Rubber Carousel, TEM Journal (10) (4) (2021) pp. 1662-1667. https://doi.org/10.18421/TEM104-23
- [4] M. Augustyn, F. Lisowski, Experimental and Numerical Studies on a Single Coherent Blade of a Vertical Axis Carousel Wind Rotor, Energies (16) (14) (2023).

"Funded by the EU NextGenerationEU through the Recovery and Resilience Plan for Slovakia under the project No. 09I03-03-V01-00131."

### **AUTHOR CONTRIBUTIONS**

- **M. Blatnický**: Conceptualization, Methodology, formal analysis, writing original draft preparation.
- **J. Dižo**: Software, Validation, Writing original draft preparation, Project administration.
- **A. Lovska:** Supervision, Review and editing, Project administration, Data curation, supervision, Investigation.
- **V. Ishchuk:** Software, Visualization, Data curation, Resources.

### DISCLOSURE STATEMENT

The authors declare that they have no known competing financial interests or personal relationships that could have appeared to influence the work reported in this paper.

### **ORCID**

**J. Dižo:** https://orcid.org/0000-0001-9433-392X

A. Lovska: https://orcid.org/0000-0002-8604-1764

**V. Ishchuk:** <a href="https://orcid.org/0000-0003-2024-382X">https://orcid.org/0000-0003-2024-382X</a>

### https://doi.org/10.3390/en16145532

- [5] M. Blatnický, J. Dižo, D. Molnár, D. Barta, Analysis of Normative Requirements and Technical Specifications in the Design of Handling Equipment for the Amusement Industry, XIX International Technical Systems Degradation Conference (2022) pp. 25-28.
- [6] National Fairground Archive. Available on: https://web.archive.org/web/20110811021142/ https://www.nfa.dept.shef.ac.uk/history/rides/history.html https://doi.org//10.13140/2.1.3104.1927
- [7] M. Blatnický, J. Dižo, D. Molnár, Structural units used in the construction of transport and handling equipment in the entertainment industry (In Slovak), Technológ (14) (2) (2022) pp. 83-86.
- [8] Y. Luo, K. Huang, S. Que, K. Chen, Cable-Carousel Structural Contact Assessment for a 10,000 Te Carousel, Proceedings of the International Offshore and Polar Engineering Conference (1) (2024), pp. 3534-3540.

- [9] R. Koňár, M. Mičian, et al., Numerical simulation of a temperature field during multibeads surface welding, Journal of Applied Mathematics and Computational Mechanics, 20 (1) (2021) pp. 49-59. https://doi.org/10.17512/jamcm.2021.1.05
- [10] H. Wen, I. Zhao, W. Chen, The Data-Driven Multivariate Process Monitoring and Diagnosis of Rides in an Amusement Park, in: Proceedings of 2018 12th IEEE International Conference on Anti-counterfeiting, Security, and Identification (ASID), Xiamen, China, 2018, pp. 136-140. https://doi.org/10.1109/ICASID.2018.8693125
- [11] A. M. Pendrill, D. Eager, Velocity, acceleration, jerk, snap and vibration: forces in our bodies during a roller coaster ride, Physics Education, 55 (2020) pp. 1-13. https://doi.org/10.1088/1361-6552/aba732
- [12] M. Blatnický, D. Molnár, V. Ishchuk, A. Suchánek, Design and Sizing of Structural Units of Technical Equipment Working in the Amusement Industry, Smart Technologies in Urban Engineering. Vol. 1: proceedings of STUE-2023, Cham: Springer Nature, pp. 255-268. <a href="https://doi.org/10.1007/978-3-031-46874-2-23">https://doi.org/10.1007/978-3-031-46874-2-23</a>
- [13] D. Molnár, M. Blatnický, J. Dižo, S. Solčanský, D. Čierňava, Analysis of Normative Requirements and Technical Specifications of a Structural Design of the Mechanical Device Operating in the Amusement Industry, Acta Technica Jaurinensis (17) (2) (2024) pp. 65-74. <a href="https://doi.org/10.14513/actatechjaur.00729">https://doi.org/10.14513/actatechjaur.00729</a>
- [14] D. Molnár, M. Blatnický, V. Ishchuk, J. Dižo, D. Čierňava, Design of a drive unit for

- technical Equipment Working in the Amusement Industry (to be published), Machine and Industrial Design in Mechanical Engineering KOD 2024.
- [15] V. Ishchuk, M. Blatnický, D. Molnár, J. Dižo, D. Čierňava, Dimensional calculation of the main beam of a technical equipment intended for the amusement industry (to be published), Machine and Industrial Design in Mechanical Engineering KOD 2024.
- [16] H. Wen, I. Zhao, W. Chen, The Data-Driven Multivariate Process Monitoring and Diagnosis of Rides in an Amusement Park, in: Proceedings of 2018 12th IEEE International Conference on Anti-counterfeiting, Security, and Identification (ASID), Xiamen, China, 2018, pp. 136-140. https://doi.org/10.1109/ICASID.2018.8693125
- [17] P. Stenzler, H. Handley, K. Woodcock, Identifying Human Factors Mismatches in Amusement Ride Containment Failure, in: P. Salmon, A. C. Macquet (Eds.), Proceedings of the Advances in Human Factors in Sports and Outdoor Recreation 2016 International Conference on Human Factors in Sports and Outdoor Recreation, Walt Disney World ®, Florida, USA, 2016, pp. 177-187. https://doi.org/10.1007/978-3-319-41953-4 16
- [18] K. N. Luttik, P. S. Anderson, L. Johanning, I. M. Viola, On the dynamics of the kite carousel, Advances in Renewable Energies Offshore -Proceedings of the 3rd International Conference on Renewable Energies Offshore, RENEW 2018, pp. 675-683.



This article is an open access article distributed under the terms and conditions of the Creative Commons Attribution NonCommercial (CC BY-NC 4.0) license.

# AJ

### ACTA TECHNICA JAURINENSIS

Vol. 17, No. 4, pp. 177-182, 2024 10.14513/actatechjaur.00753



Research Article

## Investigation of container strength when fixed in an open wagon equipped with pneumatic bags

Alyona Lovska<sup>1</sup>, Juraj Gerlici<sup>1</sup>, Ján Dižo<sup>1,\*</sup>, Pavlo Rukavishnykov<sup>2</sup>

<sup>1</sup>Department of Transport and Handling Machines, University of Žilina
Univerzitná 8215/1, 010 26 Žilina, Slovak Republic

<sup>2</sup>Department of Heat Engineering, Heat Engines and Energy Management, Ukrainian State University of
Railway Transport
Feuerbach Square 7, 61050 Kharkiv, Ukraine

\*e-mail: jan.dizo@fstroj.uniza.sk

Abstract:

Ensuring the efficiency of railway transport in international traffic needs the development of combined transport systems. Container transportation is the most relevant among them. Containers are usually transported by rail on platform wagons. Along with this, the lack of platform wagons in operation makes it necessary to use other types of wagons for container transportation, such as open wagons. The fastening of containers in open wagons is carried out using pneumatic bags. To study the effectiveness of applying such a fastening scheme, the load of the container during transportation in an open wagon was determined. The conducted research will contribute to creating recommendations for improving rail transport operations' efficiency.

Keywords: transport mechanics; container; dynamic load; container strength; container transportation

### I. Introduction

The increase in the operational efficiency of the transport industry led to the introduction of modular vehicles. Containers used in operation are one of the most common among them. This is explained by the possibility of their transportation by almost all modes of transport: rail, road, water and air [1-3]. A significant share of container transportation is accounted for the rail transport. Transportation of containers by railway is carried out on platform wagons [4-6]. The lack of platform wagons in operation makes it necessary to use other types of wagons for container transportation, for example, open wagons [7-9]. Along with this, using open wagons for container transportation requires the provision of a reliable scheme of their interaction, which would ensure their proper protection against movement during transportation.

To ensure proper fastening of containers in the longitudinal plane, pneumatic bags are found to be used there, and they are installed between the end walls of the open wagon and the container (**Fig. 1**). Usually, such pneumatic bags have standard dimensions and characteristics.





Figure 1. Transportation of containers: a) loading a container, b) fastening a container

To study the effectiveness of pneumatic bags for fastening containers in an open wagon, it is necessary to determine their load in the conditions of operational modes. Therefore, studies devoted to determining the load of a container when it is fixed in an open wagon employing pneumatic bags are relevant.

Many publications are devoted to the issue of container transportation by rail. Thus, the analysis of the main indicators of the strength of the loadbearing structure of an open wagon when transporting containers in it is described in the publication [10]. The longitudinal dynamics of an open wagon loaded with two containers were investigated. It was considered that their interaction is carried out through fitting stops, which are welded to the floor of the open wagon. The performed calculations showed that the transportation of containers using the specified fastening scheme is permissible. However, such a fastening scheme is ineffective in the conditions of over-normalized regimes. The design of a removable module of a Flat Rack type is proposed in the research [11] for an adaptation of wagons to transportation of containers. The results of the strength calculation of the removable module under the condition of its use on a platform wagon are presented. The calculation results proved the feasibility of the proposed design of the removable module.

Along with this, the authors did not investigate the possibility of its use for fastening containers in open wagons. Features of the modernization of the supporting structure of the wagon for the possibility of transporting containers on it are highlighted in the work [12]. The author's team presents the results of experimental studies of the strength of the wagon frame during a shunting collision. It was established that the proposed modernization is expedient. The features of the modernization of a freight wagon for the transportation of containers are covered in the article [13]. The authors proposed using a removable frame for placing 20-foot and 40-foot containers. It has been proven that the proposed solutions for using such a frame are effective. However, the studies [12,

13] were conducted on a platform wagon example. The paper [14] provides the solutions for the situational adaptation of open wagons to the transportation of containers. A special removable module for securing containers in an open wagon is proposed. However, when considering using such a module, the authors did not pay attention to the strength of the load-bearing structure of an open wagon and a container. The article [15] highlights the features of calculating the strength of the floor of a 40-foot container during its transportation by water transport. Recommendations for safe operation of this type of container. However, these solutions are ineffective when transporting it by rail, particularly in open wagons.

The analysis of literature sources proves that the issues of studying the load of containers during transportation by rail transport are relevant and require further research.

Regarding this, the goal of the presented research was to study the strength of a container when it is fixed in an open wagon with the help of pneumatic bags.

### II. PRESENTATION OF THE PRIMARY RESEARCH MATERIAL

Mathematical modelling was conducted to determine the efficiency of pneumatic bags for fastening containers in an open wagon. A mathematical model (1) [16] was used for this purpose. The model characterizes the load of the container in the longitudinal plane placed on the platform wagon during a shunting maneuver [17].

As part of this study, a specified model was refined by considering the force from a pneumatic bag on a container. It is assumed that the pneumatic bag is entirely distributed relative to the end wall of the container. It is considered that the container is supported and fastened in the open wagon through

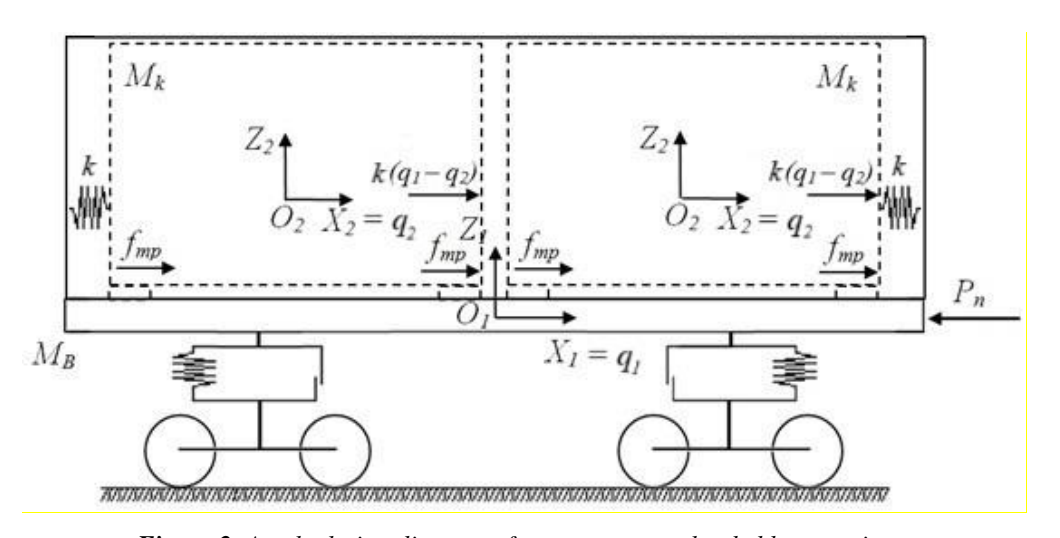


Figure 2. A calculation diagram of an open wagon loaded by containers

fittings that interact with the fitting stops. Due to a technological gap, frictional forces arise between the horizontal surfaces of fittings and fitting stops.

The container is loaded with conditional cargo using the full carrying capacity. The movement of the cargo in the container was not considered. There is no gap between the pneumatic bag and the container wall. The model did not consider the previous static compression of the pneumatic bag. The calculation diagram of an open wagon loaded by containers is shown in **Fig. 2**.

A mathematical model describing a container's dynamic load when transported in an open wagon has the following form (see Eq. (1)).

$$\begin{cases} M_{B} \cdot \ddot{q}_{1} = \\ = P_{n} - \sum_{i=1}^{n} [f_{mp} \cdot \operatorname{sign}(\dot{q}_{1} - \dot{q}_{2}) + k \\ & \cdot (q_{1} - q_{2})] \\ M_{k} \cdot \ddot{q}_{2} = \\ = f_{mp} \cdot \operatorname{sign}(\dot{q}_{1} - \dot{q}_{2}) + k \cdot (q_{1} - q_{2}), \end{cases}$$
(1)

where  $M_B$  is the wagon body mass,  $M_k$  is the container mass,  $P_n$  is the magnitude of the longitudinal force acting in an automatic coupler (the value of 3.5 MN is considered [23]), P is the stiffness of pneumatic bags,  $f_{mp}$  is the friction force (the value of 0.15, i.e. steel – steel couple is considered) between fitting stops and fittings,  $q_1$ ,  $q_2$  are generalized coordinates, at which, they are identical with the longitudinal axes  $X_1$  (for the wagon body) and  $X_2$  (for the containers). Both containers have the same coordinate system, because it is assumed that any motion is allowed between them (rigid coupling is assumed between them).

The solution for this system of equations of motion was carried out using the MathCad software [18, 19], with initial conditions set close to zero [20]. The system of equations (1) was solved using the "rkfixed" function integrated in the MathCad software. It gives velocities to individual element of

the solved mechanical system. During the calculation iteration process, the acceleration shown in Fig. 3 were obtained. The air bags stiffness value

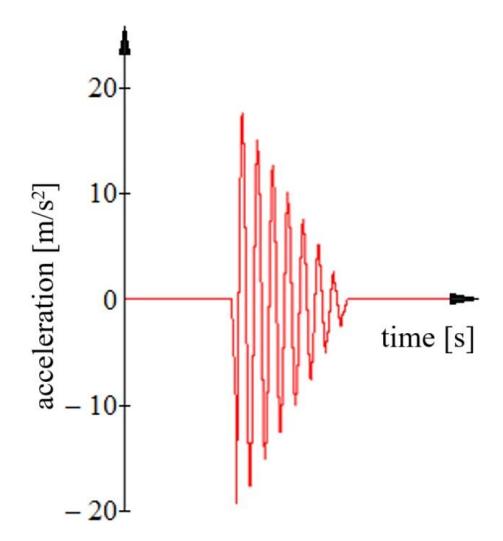


Figure 3. Accelerations acting on a container

was obtained by means of this iteration process.

The calculation results established that to maintain container accelerations up to 20 m/s<sup>2</sup>, the stiffness of the pneumatic bag should be at least 2500 kN/m (**Fig. 3**).

It is important to note, that this stiffness value should be even more important in conditions of overnormalized operating modes.

A calculation was made in SolidWorks Simulation to determine the container's strength, considering its fastening by means of pneumatic bags in the open wagon [21, 22]. The calculation diagram of the container is shown in **Fig. 4**.

This scheme considers the effect of the longitudinal load  $P_p$  on the end wall. The vertical load  $P_v$  was applied to the container's lower frame using the container's full carrying capacity, and the friction force  $f_{mp}$  was applied to the horizontal parts

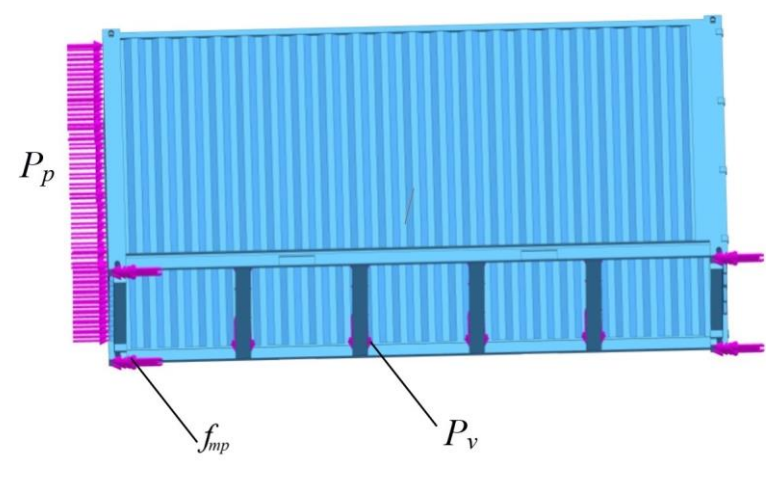


Figure 4. A calculation scheme of a container

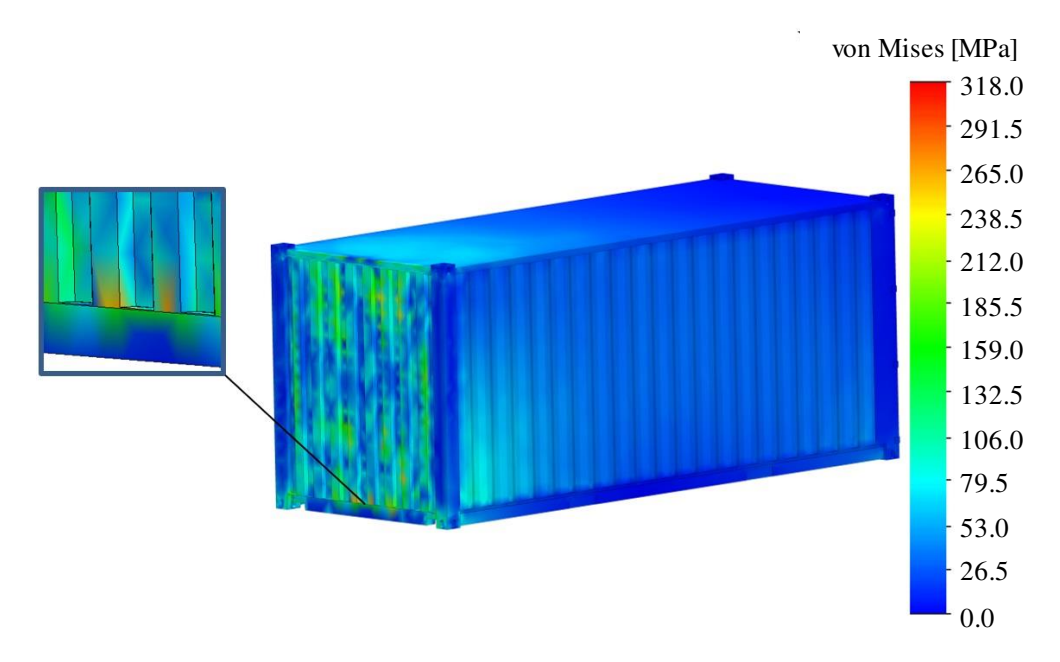


Figure 5. A stress distribution in the container structure

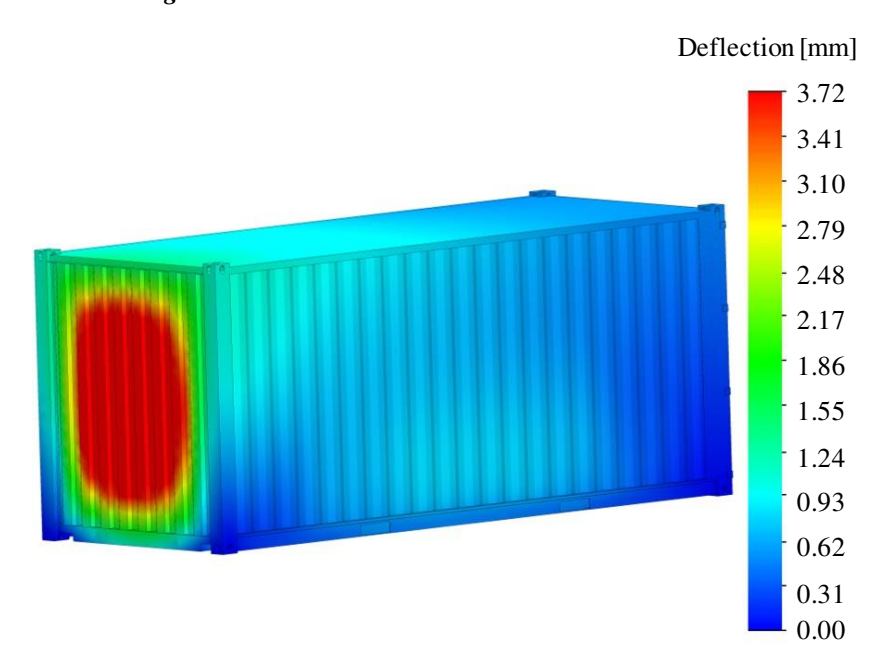


Figure 6. Deflections calculated in the container structure

of the fitting stops. The construction material is 09G2S steel. The permissible strength of the used material is of 310.5 MPa [23].

### III. RESULTS OF THE STRENGTH ANALYSIS OF THE CONTAINER

The finite element model of the container is formed by tetrahedral elements. Their optimal number was determined by the graphic-analytical method [24]. The calculation results are shown in **Fig. 5** and **Fig. 6**.

The maximum stresses in the container were identified in the area where the cladding adhered to the end beam of the container and mounted. It is also detailed in **Fig. 5**.

These values were up to 318.0 MPa. The maximum deflections detected in the end wall occur at its center and are equal to the value of 3.7 mm, as seen in **Fig. 6**. The calculation results allow to conclude that the strength of the container under the applied loads is not ensured.

The research proved that applying the pneumatic bags led to an excessive load on the container in the

open wagon. Future research will focus on improving the proposed idea through improving the structure. Subsequently, strength analyses will be performed to determine whether using pneumatic bags is possible.

### IV. CONCLUSION

Mathematical modeling of the longitudinal load of a container placed in an open wagon was carried out. It was established that to maintain container accelerations within  $20~\text{m/s}^2$ , the stiffness of the pneumatic bag should be at least 2,500~kN/m.

The strength of the container is calculated when it is fixed in the open wagon with the help of pneumatic bags. The maximum stresses in the container were identified in the area where the cladding adhered to the end beam of the container and amounted to the value of 318.0 MPa. The maximum deflections in the end wall occur at its center. These deflections were numbered to the value of 3.7 mm. Based on the calculation results, it is possible to conclude that the required strength of the container under the acting loads has not been met. Therefore, the issue of improving the scheme of securing containers in open wagons requires further research.

### ACKNOWLEDGEMENT

This research was also supported by the Slovak Research and Development Agency of the Ministry of Education, Science, Research and Sport of the Slovak Republic VEGA 1/0308/24 "Research of dynamic properties of rail vehicles mechanical systems with flexible components when running on a track.

This publication was supported by the Cultural and Educational Grant Agency of the Ministry of

### REFERENCES

- [1] M. Milenković, N. Bojović, D. Abramin, Railway freight wagon fleet size optimization: A real-world application, Journal of Rail Transport Planning and Management 26 (2023).
  - https://doi.org/10.1016/j.jrtpm.2023.100373
- [2] J. Li, K. Jing, M. Khimich, L. Shen, Optimization of green containerized grain supply chain transportation problem in Ukraine considering disruption scenarios, Sustainability 15 (9) (2023) pp. 1-21. https://doi.org/10.3390/su15097620
- [3] J. Široky, P. Nachtigall, E. Tischer, K. Schejbal, T. Michalek, The modelling of traction energy consumption of a container train, Transportation Research Procedia 77 (2024) pp. 76-84. https://doi.org/10.1016/j.trpro.2024.01.010

Education of the Slovak Republic in the project KEGA 031ŽU-4/2023: Development of key competencies of the graduate of the study program Vehicles and Engines.

"Funded by the EU NextGenerationEU through the Recovery and Resilience Plan for Slovakia under the project No. 09I03-03-V01-00131."

### **AUTHOR CONTRIBUTIONS**

- **A. Lovska**: Conceptualization, Methodology, Software, Writing original draft preparation, visualization.
- **J. Gerlici**: Formal analysis, Investigation, Supervision, Validation.
- **J. Dižo**: Writing original draft preparation, Project administration, Data curation.
- **P. Rukavishnykov**: Resources, Formal analysis, Visualisation.

### **DISCLOSURE STATEMENT**

The authors declare that they have no known competing financial interests or personal relationships that could have appeared to influence the work reported in this paper.

### **ORCID**

- **A. Lovska** https://orcid.org/0000-0002-8604-1764
- J. Gerlici https://orcid.org/0000-0003-3928-0567
- J. Dižo https://orcid.org/0000-0001-9433-392X
- **P. Rukavishnykov** <a href="https://orcid.org/0000-0002-9670-3071">https://orcid.org/0000-0002-9670-3071</a>
- [4] F. Haferkorn, Articulated train of deep well cars for high-speed container transport, WIT Transactions on the Built Environment 213 (2022) pp. 121-134. https://doi.org/10.2495/CR220111
- [5] I. Medvediev, D. Muzylyov, J. Montewka, A model for agribusiness supply chain risk management using fuzzy logic. Case study: Grain route from Ukraine to Poland, Transportation Research Part E: Logistics and Transportation Review 190 (2024) pp. 1-27. https://doi.org/10.1016/j.tre.2024.103691
- [6] D. Wang, Ch. Xie, A descriptive and prescriptive analysis of rail service subsidies in the China–Europe freight transportation market, International Journal of Transportation Science and Technology (2024) pp. 1-16. https://doi.org/10.1016/j.ijtst.2024.06.003

- [7] R. Zaripov, P. Gavrilovs, Research opportunities to improve technical and economic performance of freight car through the introduction of lightweight materials in their construction, Procedia Engineering 187 (2017), pp. 22-29. https://doi.org/10.1016/j.proeng.2017.04.345
- [8] K. Bizoń, A. Chmielewska, A. Chudzikiewicz, A. Sładkowski, A. Stelmach, Integrated research of multi-purpose stanchion baskets for transporting timber and containers, Transport Problems 18 (4) (2023) pp. 73-86. https://doi.org/10.20858/tp.2023.18.4.06
- [9] A. Das, G. Agarwal, Investigation of Torsional Stability and Camber Test on a Meter Gauge Flat Wagon, Lecture Notes in Mechanical Engineering (2020) pp. 271-280. https://doi.org/10.1007/978-981-15-0772-4 24
- [10] A. Lovska, J. Dižo, A. Rybin, P. Rukavishnykov, Features of determining the strength indicators of an open wagon body when transporting containers in it (In Ukrainian), Scientific News of Dahl University 26 (2024) pp. 1-6, in Ukrainian. https://doi.org/10.33216/2222-3428-2024-26-9
- [11] S. Panchenko, J. Gerlici, G. Vatulia, A. Lovska, M. Pavliuchenkov, K. Kravchenko, the analysis of the loading and the strength of the FLAT RACK removable module with viscoelastic bonds in the fittings, Applied Sciences 13 (1) (2023) pp. 1-14. https://doi.org/10.3390/app13010079
- [12] O. H. Reidemeister, V. O. Kalashnyk, O. A. Shykunov, Modernization as a way to improve the use of universal cars, Science and Transport Progress 2 (62) (2016) pp. 148-156. https://doi.org/10.15802/stp2016/67334
- [13] V. Shaposhnyk, O. Shykunov, A. Reidemeister, M. Leontii, O. Potapenko, Determining the possibility of using removable equipment for transporting 20- and 40-feetlong containers on an universal platform wagon, Eastern-European Journal of Enterprise Technologies 1 (7) (2021) pp. 14-21. <a href="https://doi.org/10.15587/1729-4061.2021.225090">https://doi.org/10.15587/1729-4061.2021.225090</a>
- [14] J. Gerlici, A. Lovska, G. Vatulia, M. Pavliuchenkov, O. Kravchenko, S. Solcansky, Situational adaptation of the open wagon body to container transportation, Applied Sciences 13 (15) (2023) pp. 1-19. https://doi.org/10.3390/app13158605
- [15] A. Rzeczycki, B. Wiśnicki, Strength Analysis of shipping container floor with Gooseneck

- tunnel under heavy cargo load, Solid State Phenomena 252 (2016) pp. 81-90. https://doi.org/10.4028/www.scientific.net/SSP.252.81
- [16] A. Lovska, Determination of the load of a container placed on a platform car during the elastic-viscous interaction of fittings with fitting stops, Collection of scientific works of UkrSURT 184 (2019), pp. 6-19, in Ukrainian.
- [17] Y. Q. Sun, M. Spiryagin, Q. Wu, C. Cole, Lateral instability of three-piece bogie container wagon and effect of the loading distributions, Proceedings of the Institution of Mechanical Engineers, Part F: Journal of Rail and Rapid Transit 238 (4) (2024) pp. 370-380. https://doi.org/10.1177/09544097231183
- [18] I. V. Bohach, O. Yu. Krakovetskyi, L. V. Kylyk, Numerical methods for solving differential equations using MathCad, Tutorial, Vinnytsia, VNTU (2020), 106 p., in Ukrainian.
- [19] A. V. Syasev, Introduction to the MathCad system: a study guide, Dnipropetrovsk, Publishing House of Dnipropetr. University (2004) 108 p., in Ukrainian.
- [20] A. Lovskaya, Assessment of dynamic efforts to bodies of wagons at transportation with railway ferries, Eastern-European Journal of Enterprise Technologies 3 (4) (2014) pp. 36-41. <a href="https://doi.org/10.15587/1729-4061.2014.24997">https://doi.org/10.15587/1729-4061.2014.24997</a>
- [21] S. I. Pustylga, V. R. Samostyan, Y. V. Klak, Engineering graphics in SolidWorks: a tutorial, Lutsk, Tower (2018) 172 p., in Ukrainian.
- [22] M. M. Kozyar, Yu. V. Feshchuk, O. V. Parfenyuk, Computer graphics: SolidWorks: Study guide, Kherson, Oldi-plus (2018) 252 p., in Ukrainian.
- [23] DSTU 7598:2014. Freight wagons. General requirements for calculations and design of new and modernized 1520 mm gauge wagons (non-self-propelled) Kyiv (2015) 250 p., in Ukrainian.
- [24] A. Lovska, O. Stanovskyi, O. Zharova, Y. Naumenko, Y. Pelypenko, Identifying patterns in loading a gondola car body with reinforcing belts in the structure of side walls, Eastern-European Journal of Enterprise Technologies 3 (7) (2024) pp. 17-25. https://doi.org/10.15587/1729-

https://doi.org/10.15587/1729-4061.2024.303987



This article is an open access article distributed under the terms and conditions of the Creative Commons Attribution NonCommercial (CC BY-NC 4.0) license.

# AJ

### **ACTA TECHNICA JAURINENSIS**

Vol. 17, No. 4, pp. 183-187, 2024 10.14513/actatechjaur.00759



Research Article

### Compact Defected Ground Structure Microstrip Patch Antenna for Wi-Fi Applications

### Dipak Omprakash Sakle<sup>1,\*</sup>, Manish P Deshmukh<sup>2</sup>

<sup>1</sup>Department of Electronics and Telecommunication Engineering, SSBTCOE&T Bambhori, Jalgaon 425001, India 
<sup>2</sup>Department of Electronics and Telecommunication Engineering, SSBTCOE&T Bambhori, Jalgaon 425001, India 
\*e-mail: dipak.sakhala@gmail.com

Abstract:

In recent years microstrip patch antennas having minute size is an exciting topic for many researchers and design engineers. In this paper a novel miniaturized microstrip patch antenna for Wi-Fi applications is proposed. The concept of defected ground plane (DGS) is used for achieving miniaturization. The prototype is designed and analyzed by CST Microwave Studio. Low cost FR-4 substrate having thickness of  $0.8\,$  mm is used for the design of the antenna. The antenna is having compact size of  $16\times17\,$  mm². The simulated results demonstrate that the antenna has bandwidth of 2.02% (49 MHz) with -41.46 dB reflection coefficient at resonating frequency. The antenna has bidirectional radiation pattern. The proposed design provides a size reduction of 75.46% in comparison to conventional patch. The proposed antenna is having compact size and is low cost which makes it a suitable candidate for  $2.4\,$  GHz Wi-Fi band.

Keywords: Wi-Fi; microstrip antenna; DGS; miniaturization; slot

### I. Introduction

Wireless technology has developed rapidly in recent years, making cellular communication more advanced than ever [1]. It has revolutionized our lives, our jobs, and how we interact with one another. When it comes to wireless communication, an antenna plays a vital role. Due to the stringent requirements of modern communication systems, miniaturized antennas have become increasingly popular [2]. Due to their complexity and restrictions, designing a compact antenna becomes a crucial task for scientists and researchers [3]. Recent years have seen an increase in the use of microstrip patch antennas due to their low cost, light weight, inexpensive and easy manufacturing using printed circuit boards [4-5].

In [5] authors presented a detailed review of topology- and material-based methods for miniaturization of antenna. The topology-based miniaturization techniques include the defected ground structure. Microstrip antennas that integrate defected ground structures (DGS) have become increasingly popular thanks to their simple structural designs and ease of imprinting on microstrip substrates [6].

Slot on the patch affects the input impedance matching and degrade pattern purity. It can be prevented by employing slots on the ground plane known as defected ground structure (DGS). In comparison to slot on the patch DGS provides better results in terms of frequency and cross-polar (XP) level [7]. As a result of the modification to the ground plane, a discontinuity has occurred in the ground plane, which has caused the primary radiator's electric current to reroute along the ground's conducting surface, thus increasing the ground plane's electrical length [5, 8]. In addition to reduce the antenna size DGS is integrated in patch antenna for various applications like harmonic suppression, cross-polarization reduction [9] and mutual coupling reduction [10].

Each DGS shape has its own characteristics and creates effect on the performance of the device according to its geometry and size. Effective capacitance and effective inductance of the model are changed by embedding the slots on the ground plane, resulting in shifting of resonance frequency to its lower side. Thus, compactness is achieved by using DGS [11].

By introducing DGS antenna resonance frequency is shifted from 5.7 GHz to 3 GHz resulting in size reduction up to 50% [10]. For lower GNSS, WiMAX, C-band and WLAN systems a compact multiband antenna utilizing slot in the radiating patch and the ground plane is addressed in [12]. A miniaturized quadband heart-shaped planar monopole antenna (QHPMA) by using the combination of the DGS, and the metallic vias is presented in [13]. For LoRa application at 868 MHz an inset fed miniaturized antenna with defected ground plane is proposed [14]. Here linearly polarized waves are generated. Using defected ground structure, a miniaturized microstrip patch antenna array is demonstrated in [15], for S band at 2.2 GHz with size reduction up to 83% in comparison to conventional patch antenna. A circularly polarized triple band microstrip fed simple square slot antenna is presented in [16] for S-band and C-band.

Based on the literature presented above, it is evident that by using the concept of defected ground plane miniaturized microstrip patch antennas have been designed for various different wireless applications, these antennas can be single band, multi band antennas or they can be reconfigurable one. The main purpose of this work is to design and analyse a miniaturized microstrip patch antenna with defect in the ground plane. A novel shape of DGS is proposed which results in the antenna to operate at 2.4 GHz Wi-Fi band. CST microwave studio [17] is used for the design and analysis of the proposed antenna.

The rest of the paper is organized as follows. In section II the methodology for the designing of the proposed miniature antenna loaded with DGS is discussed. Section III deals with the discussion of simulation results. Finally, section IV concludes the paper.

### II. DESIGN METHODOLOGY

The main purpose of this work is to design a compact antenna for Wi-Fi applications using DGS method. This section describes the design methodology of the proposed antenna. The geometry of the proposed antenna is shown in **Fig.1**. As shown modifications are done in the ground plane which results in the discontinuity in the ground surface

current path. The defect in the ground plane alters the electrical length of the ground plane and the antenna starts resonating at lower resonant frequency.

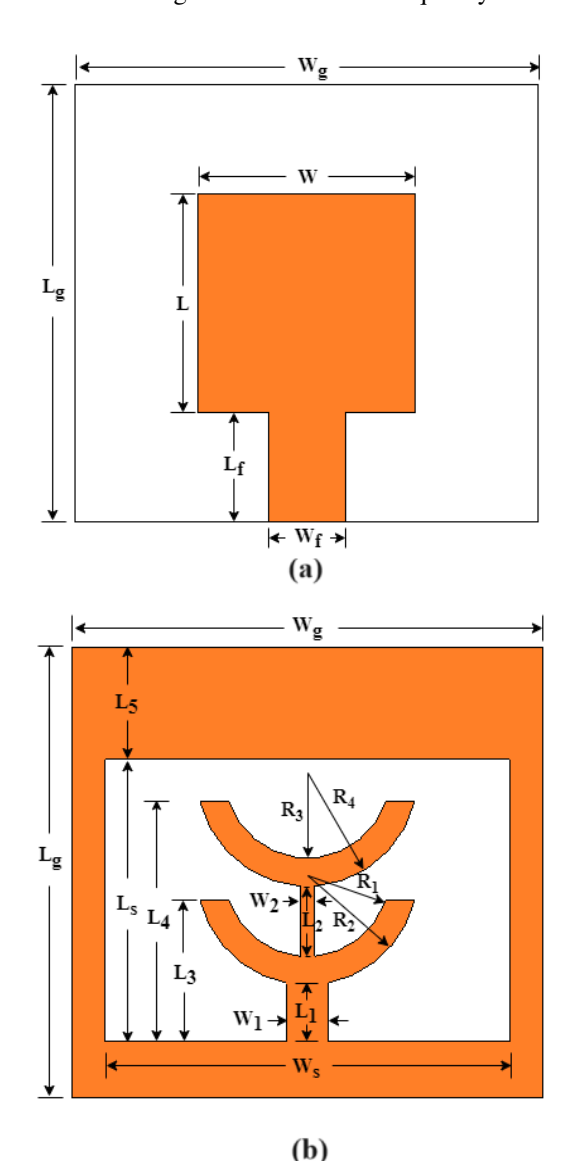


Figure 1. Antenna geometry (a) front view and (b) back view.

As shown in **Fig.1** the top layer of the antenna consists of square radiating patch and the ground plane is having defected structure. The square patch is fed with 50  $\Omega$  microstrip feed-line. The antenna is printed on low cost FR-4 substrate having thickness

Table 1. Dimensions of the proposed antenna (mm).

Parameter	Value	Parameter	Value	Parameter	Value	Parameter	Value
$L_{g}$	16	$L_{\mathrm{f}}$	4	$L_2$	2.5	$\mathbf{W}_2$	0.5
$\mathbf{W}_{g}$	17	$\mathbf{W}_{\mathrm{f}}$	3	$L_3$	5	$\mathbf{R}_1$	3
$\mathbf{H}_{\mathrm{s}}$	0.8	$L_{s}$	10	$L_4$	8.5	$\mathbf{R}_2$	4
L	8	$\mathbf{W}_{\mathrm{s}}$	14.6	$L_5$	4	$R_3$	3
W	8	$L_1$	2	$\mathbf{W}_1$	1.5	$R_4$	4

of 0.8 mm, dielectric constant of 4.4 and loss tangent of 0.02. The overall size of the antenna is  $L_g \times W_g \times H_s = 16 \times 17 \times 0.8 \text{ mm}^3$ . The optimized design parameters of the proposed antenna are listed in Table 1. The size reduction achieved is 75.46% in comparison to conventional patch. With the proposed design, we aim to create a compact, low cost antenna for Wi-Fi applications. The design strategy was to keep the reflection coefficient (S\_{11}) of less than -10 dB.

### III. RESULTS AND DISCUSSIONS

To study the performance of the proposed microstrip patch antenna, the antenna prototype is designed, simulated, and analyzed using CST microwave studio.

In order to understand the influence of the various design parameters on the resonant frequency of the antenna parametric analysis is necessary. Parametric analysis is performed by varying one parameter at a time and keeping other as constant. The vital parameters selected for analysis are  $W_1$  and  $W_2$ .

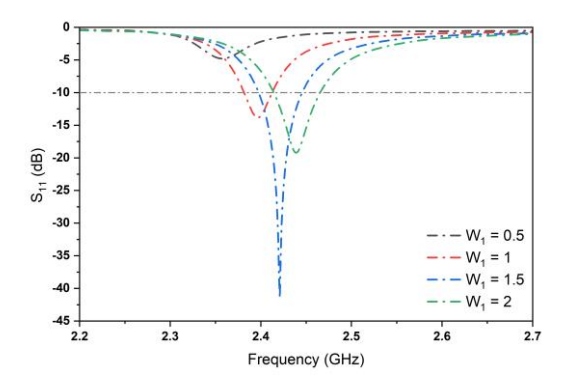


**Figure 2.** Effect of variation in  $W_1$  on the reflection coefficient  $(S_{11})$ .

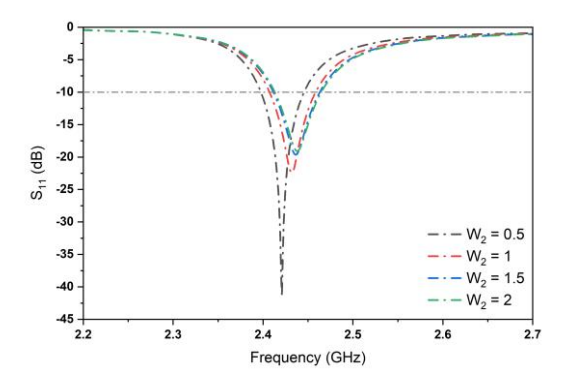


**Figure 3.** Effect of variation in  $W_2$  on the reflection coefficient  $(S_{11})$ .

The effect of width  $W_1$  on the performance of the antenna is studied first. The width  $W_2$  is kept constant at 0.5 mm and the width  $W_1$  is varied from 0.5 mm to 2 mm in suitable steps. The effect of variation in  $W_1$  on the reflection coefficient is shown

in **Fig.2**. As can be seen from the figure as the width  $W_1$  increases, the resonant frequency increases significantly. When  $W_1$  equals to 1.5 mm the antenna resonates at 2.42 GHz with reflection coefficient equals -41.46 dB.

**Fig.3** shows the effect of variation on the reflection coefficient for different values of  $W_2$  keeping  $W_1$  constant at 1.5 mm. The width  $W_2$  is varied from 0.5 mm to 2 mm in suitable steps. As the value of  $W_2$  increases, the frequency shifts from 2.42 GHz to 2.44 GHz with reduction in reflection coefficient from -41.46 dB to -19.09 dB.

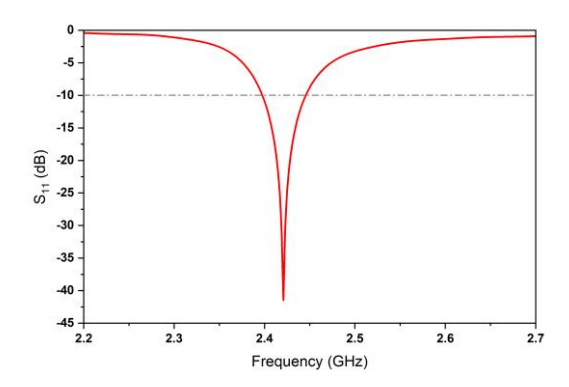


**Figure 4.** Simulated reflection coefficient  $(S_{11})$  of the proposed antenna.

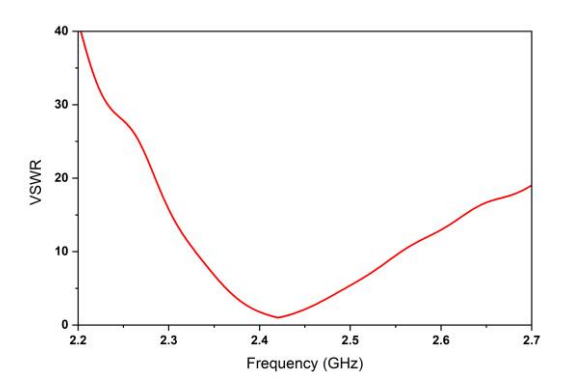


**Figure 5.** Simulated VSWR of the proposed antenna.

**Fig.4** shows the reflection coefficient of the proposed antenna. The simulated results show that the antenna resonate at 2.42 GHz with reflection coefficient ( $S_{11}$ ) of -41.46 dB and has bandwidth of 2.02% (2.397-2.446 GHz). For efficient performance of the antenna the value of VSWR should be between 1 and 2. The VSWR plot is shown in **Fig.5**. At the operating frequency the antenna has VSWR value of 1.01.

The simulated normalized radiation patterns of the proposed patch antenna including the copolarization and cross-polarization in the H-plane ( $\phi$  = 0) and E-plane ( $\phi$  = 90) are shown in **Fig.6**. The proposed antenna produces almost symmetrical

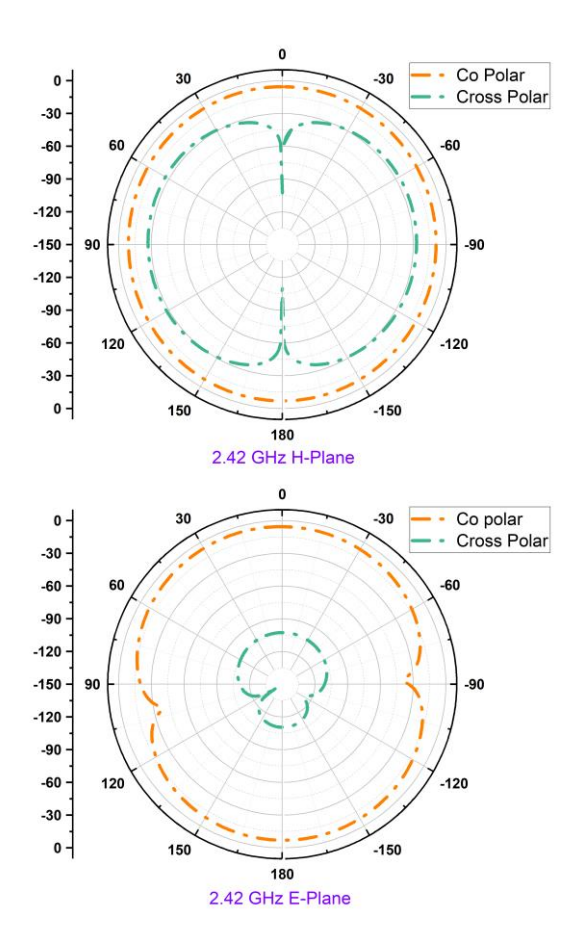


**Figure 6.** Simulated normalized radiation patterns of the proposed antenna.

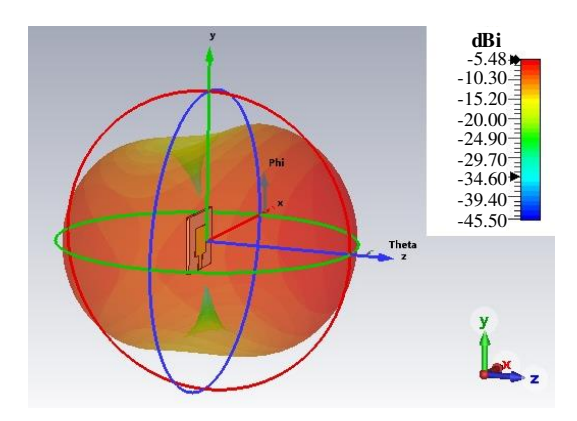


**Figure 7.** Simulated 3D radiation pattern of the proposed antenna.

radiation pattern having bidirectional nature. In the proposed design the E-plane and H-plane cross-polarization levels are lower than that of the co-polarization levels. The 3D radiation pattern of the proposed antenna at 2.42 GHz is shown in **Fig. 7**. The simulated gain of the antenna is -5.48 dBi.

For further analysis, we have investigated surface current impact on the performance of the antenna. **Fig.8** shows the average surface current distribution on both the patch and the ground plane of the proposed antenna. As can be seen in figure the

intensity of current on the defected ground plane is very high in comparison to the patch. The figure also shows the current path on the top surface is along the microstrip line to the edges of the square patch and then the current shifts to the ground plane from the top of the DGS towards its bottom completing its path. In this way the DGS affects the ground plane's electrical length and the antenna is able to radiate at lower frequency.



Figure 8. Current distribution of patch antenna with DGS, (a) front view, (b) back view.

### IV. CONCLUSION

A miniaturized microstrip patch antenna fed by microstrip feed line is proposed. Modifications are done on the ground plane to achieve the miniature size. The antenna operates at 2.42 GHz with reflection coefficient of -41.46 dB. Detailed analysis is carried out to investigate the effect of vital parameters on the design of antenna. The design provides substantial reduction in size as compared to a typical microstrip patch antenna operating at the same frequency. The antenna is having miniature size to be installed in communication systems where available space is a major issue.

### **AUTHOR CONTRIBUTIONS**

**D. Sakle**: Conceptualization, Theoretical analysis, Antenna simulation, Writing, Review and editing.

M. Deshmukh: Supervision, Review and editing.

### **DISCLOSURE STATEMENT**

The authors declare that they have no known competing financial interests or personal relationships that could have appeared to influence the work reported in this paper.

### **ORCID**

If the authors have ORCID identification, it must be given in this section.

D. Sakle <a href="https://orcid.org/0000-0002-7234-2574">https://orcid.org/0000-0002-7234-2574</a>

**M. Deshmukh** <a href="https://orcid.org/0009-0001-2557-2596">https://orcid.org/0009-0001-2557-2596</a>

### REFERENCES

- [1] S. L. Mallikarjun, P. M. Hadalgi, Study on effect of defective ground structure on hybrid microstrip array antenna, Wireless and Mobile Technologies 1 (1) (2013) pp. 1-5. https://doi.org/10.12691/wmt-1-1-1
- [2] R. Patel, A. Desai, T. K. Upadhyaya, An electrically small antenna using defected ground structure for RFID, GPS and IEEE 802.11 a/b/g/s applications, Progress In Electromagnetics Research Letters 75 (2018) pp. 75–81. https://doi.org/10.2528/PIERL18021901
- [3] D. N. Gençoğlan, Ş. Çolak, M. Palandöken, Spiral-resonator-based frequency reconfigurable antenna design for sub-6 GHz applications, Applied Sciences 13 (15) (2023) pp. 1-21. https://doi.org/10.3390/app13158719
- [4] M. R. Ahsan, M. T. Islam et al., Compact double-P slotted inset-fed microstrip patch antenna on high dielectric substrate, The Scientific World Journal 2014 (1) (2014) pp. 1-6. https://doi.org/10.1155/2014/909854
- [5] M. Fallahpour, R. Zoughi, Antenna miniaturization techniques: A review of topology- and material-based methods, in IEEE Antennas and Propagation Magazine 60 (1) (2017) pp. 38-50. https://doi.org/10.1109/MAP.2017.2774138
- [6] L. M. Therase, T. Jayanthy, A novel microstrip antenna using circular ring defected ground structure for X band applications, Measurement 183 (2021). https://doi.org/10.1016/j.measurement.2021.1 09768
- [7] P. A. Kadam, A. A. Deshmukh, Variations of compact rectangular microstrip antennas using defected ground plane structure, Journal of Microwaves, Optoelectronics and Electromagnetic Applications 21 (2) (2022) pp. 265-283. <a href="https://doi.org/10.1590/2179-10742022v21i2256950">https://doi.org/10.1590/2179-10742022v21i2256950</a>
- [8] N. Ojaroudi Parchin, H. Jahanbakhsh Basherlou et al., Multi-band MIMO antenna design with user-impact investigation for 4G and 5G mobile terminals, Sensors 19 (3) (2019). https://doi.org/10.3390/s19030456

- [9] K. Suvarna, N. R. Murty, D. V. Vardhan, A miniature rectangular patch antenna using defected ground structure for WLAN applications, Progress In Electromagnetics Research C 95 (2019) pp. 131–140. https://doi.org/10.2528/PIERC19061602
- [10] H. Elftouh, N. A. Touhami et al., Miniaturized microstrip patch antenna with defected ground structure, Progress In Electromagnetics Research C 55 (2014) pp. 25-33. https://doi.org/10.2528/PIERC14092302
- [11] M. K. Khandelwal, B. K. Kanaujia, S. Kumar, Defected ground structure: fundamentals, analysis, and applications in modern wireless trends, International Journal of Antennas and Propagation 2017 (1) (2017). <a href="https://doi.org/10.1155/2017/2018527">https://doi.org/10.1155/2017/2018527</a>
- [12] I. Khan, T. Ali, G. D. Devanagavi et al., A compact multiband band slot antenna for wireless applications, Internet Technology Letters 2 (6) (2019). <a href="https://doi.org/10.1002/itl2.94">https://doi.org/10.1002/itl2.94</a>
- [13] P. M. Mpele, F. M. Mbango et al., A novel quadband ultra miniaturized planar antenna with metallic vias and defected ground structure for portable devices, Heliyon 7 (3) (2021). https://doi.org/10.1016/j.heliyon.2021.e06373
- [14] A. Pandey, M. V. D. Nair, Inset fed miniaturized antenna with defected ground plane for LoRa applications, Procedia Computer Science 171 (2020) pp. 2115-2120. https://doi.org/10.1016/j.procs.2020.04.228
- [15] R. A. Pandhare, P. L. Zade, M. P. Abegaonkar, Miniaturized microstrip antenna array using defected ground structure with enhanced performance, Engineering science and technology, an international journal 19 (3) (2016) pp.1360-1367. <a href="https://doi.org/10.1016/j.jestch.2016.03.007">https://doi.org/10.1016/j.jestch.2016.03.007</a>
- [16] H. K. Behera, M. Midya, L. P. Mishra, Triple band dual sense circularly polarized slot antenna for s and c band applications, Progress In Electromagnetics Research C 132 (2023) pp. 217-229. https://doi.org/10.2528/pierc23022101
- [17] CST Microwave Studio (2021). https://www.3ds.com/products/simulia/cst-studio-suite



This article is an open access article distributed under the terms and conditions of the Creative Commons Attribution NonCommercial (CC BY-NC 4.0) license.